Published in final edited form as:

Neuron. 2017 October 11; 96(2): 373–386.e6. doi:10.1016/j.neuron.2017.09.034.

Paclitaxel reduces axonal Bclw to initiate IP_3R1-dependent axon degeneration

Sarah E. Pease-Raissi[1,2,4], **Maria F. Pazyra-Murphy**[1,2,4], **Yihang Li**[1,2], **Franziska Wachter**[2,3], **Yusuke Fukuda**[1,2], **Sara J. Fenstermacher**[1,2], **Lauren A. Barclay**[2,3], **Gregory H. Bird**[2,3], **Loren D. Walensky**[2,3], and **Rosalind A. Segal**[1,2,*]

[1]Department of Neurobiology, Harvard Medical School, Boston, MA 02115, USA

[2]Departments of Cancer Biology and Pediatric Oncology, Dana-Farber Cancer Institute, Boston, MA 02115, USA

[3]Linde Program in Cancer Chemical Biology, Dana-Farber Cancer Institute, Boston, MA 02215, USA

Summary

Chemotherapy induced peripheral neuropathy (CIPN) is a debilitating side effect of many cancer treatments. The hallmark of CIPN is degeneration of long axons required for transmission of sensory information; axonal degeneration causes impaired tactile sensation and persistent pain. Currently the molecular mechanisms of CIPN are not understood, and there are no available treatments. Here we show that the chemotherapeutic agent paclitaxel triggers CIPN by altering IP_3 receptor phosphorylation and intracellular calcium flux, and activating calcium-dependent calpain proteases. Concomitantly paclitaxel impairs axonal trafficking of RNA-granules and reduces synthesis of Bclw (*bcl2l2*), a Bcl2 family member that binds IP_3R1 and restrains axon degeneration. Surprisingly, Bclw or a stapled peptide corresponding to the Bclw BH4 domain interact with axonal IP_3R1 and prevent paclitaxel-induced degeneration, while Bcl2 and $Bclx_L$ cannot do so. Together these data identify a Bclw-IP_3R1-dependent cascade that causes axon degeneration, and suggest Bclw-mimetics could provide effective therapy to prevent CIPN.

*Correspondence: rosalind_segal@dfci.harvard.edu (Lead Contact).
[4]These authors contributed equally to this work.

Author contributions

S.E.P.-R., M.F.P.-M., Y.L., S.J.F., R.A.S., and L.D.W. designed research
S.E.P.-R., M.F.P.-M., Y.L., F.W., Y.F., L.A.B., and G.H.B. performed research
S.E.P.-R., M.F.P.-M., Y.L., and F.W. analyzed data
S.E.P.-R., M.F.P.-M., and R.A.S wrote the paper with input from L.D.W., F.W., and Y.L.

L.D.W. is a scientific advisory board member and consultant for Aileron Therapeutics.

Introduction

Axons that span long distances enable rapid communication within a neural circuit, but they are particularly vulnerable to degeneration. Axonal degeneration is a key feature of both neuronal pruning during development and of diverse neuropathological disorders. Molecular cascades governing pathological degeneration exhibit both commonalities with and differences from developmental axon degenerative cascades (Pease and Segal, 2014; Wang et al., 2012). Pathological axon degeneration involves aberrant calcium signaling, changes in mitochondrial function, and activation of calpain proteases. Bcl2 family members, which are implicated in developmental axon pruning (Cosker et al., 2016; Cosker et al., 2013; Courchesne et al., 2011; Pazyra-Murphy et al., 2009; Schoenmann et al., 2010; Simon et al., 2016; Simon et al., 2012; Vohra et al., 2010), are capable of regulating mitochondrial morphology and calcium homeostasis (Chipuk et al., 2010). However, it is not yet known if pathological axon degeneration involves Bcl2 components. Therapies targeting Bcl2 family members exhibit great promise in preclinical and clinical studies (Anderson et al., 2016; Bodur and Basaga, 2012; Konopleva et al., 2016; LaBelle et al., 2012; Walensky et al., 2004; Weyhenmeyer et al., 2012), and so identification of Bcl2 family members involved in axon degenerative processes could provide a molecular handle to understand and prevent pathological degenerative cascades.

Many cancer therapies cause axon injury and neurological impairment, resulting in Chemotherapy- induced peripheral neuropathy (CIPN). In patients with CIPN, degeneration of long peripheral sensory or motor neuron axons causes pain, tingling, numbness, and/or impaired motor function.

Chemotherapeutic drugs that cause CIPN include platinum drugs, vinca alkaloids, and taxanes such as paclitaxel. Paclitaxel, a microtubule stabilizing agent commonly used to treat patients with breast, ovarian, lung, or other cancers, causes a primarily sensory neuropathy (Gornstein and Schwarz, 2014). It has been suggested that paclitaxel elicits a degenerative cascade similar to that observed after mechanical axon injury (Fukuda et al., 2017; Gornstein and Schwarz, 2014; Wang et al., 2002; Wang et al., 2004). However, the molecular mechanism for paclitaxel-induced degeneration is not understood, and there are currently no treatments available for this common disorder. As CIPN often necessitates reducing the dose of chemotherapeutic drugs, it both limits the ability to treat many cancers and also causes severe disability for cancer survivors.

Here we use *in vitro* and *in vivo* systems to analyze the pathological effects of paclitaxel on dorsal root ganglia (DRG) sensory neurons. Our data indicate that paclitaxel acts directly on axons of sensory neurons to alter inositol 1,4,5-trisphosphate receptor (IP_3R) activity and initiate axon degeneration. We show that paclitaxel treatment selectively reduces axonal expression of the Bcl2 family member Bclw (Bcl2l2) by impairing axonal trafficking of RNA transport granules containing *bclw* mRNA and the RNA-binding protein SFPQ, and thus inhibiting *bclw* translation. Moreover, the BH4 domain of Bclw binds IP_3R1 and thereby prevents paclitaxel-induced axonal degeneration, a function that is not shared by Bcl2 or $Bclx_L$. Together these findings identify a mechanism for CIPN and demonstrate that the underlying axonal degenerative process partially overlaps with critical cascades triggered

by developmental pruning or traumatic injury. Importantly, these studies suggest that Bclw BH4-mimetics may provide a clinically useful preventative therapy for CIPN and other disorders of axonal degeneration.

Results

Paclitaxel causes axon fragmentation and initiation of an axon degenerative cascade

While recent reports suggest paclitaxel acts directly on axons to reduce axon length (Yang et al., 2009) and impair outgrowth (Gornstein and Schwarz, 2017), it is not yet established whether paclitaxel directly impacts sensory axons to cause degeneration, or whether degeneration represents an indirect consequence of paclitaxel affecting other components of the sensory circuitry (Jin et al., 2008; Kiya et al., 2011; Li et al., 2014; Peters et al., 2007a; Peters et al., 2007b; Yang et al., 2009; Zhang et al., 2012). To determine the subcellular site of action for paclitaxel-induced degeneration, we introduced paclitaxel (30 nM) into the media surrounding either cell body or distal axon compartments of E15 DRG sensory neurons in compartmented cultures, and analyzed paclitaxel-induced axonal fragmentation, a direct readout of degeneration (Sasaki et al., 2009). We find that paclitaxel added to axons increases axon degeneration, while paclitaxel added to cell bodies has no effect (Figure 1A and 1B). Notably, paclitaxel treatment of either subcellular compartment did not induce cell body apoptosis as assessed by nuclear condensation (Figure 1C and 1D).

Following traumatic axon injury, calcium dysregulation is a critical step that alters mitochondrial function and activates calpain proteases to induce axon degeneration (Barrientos et al., 2011; Villegas et al., 2014; Wang et al., 2012). Similarly, paclitaxel applied to axons reduced both axonal mitochondrial membrane potential as assessed by the voltage-sensitive dye TMRE (Figure 1E) and axonal mitochondrial length (Figure 1F and 1G; average axonal mitochondrial length 0.92 ± 0.01 μm (DMSO), 0.7 ± 0.04 μm (paclitaxel), $p < 0.05$ by Student's *t*-test), and also increased calpain activity in a dose-dependent manner (Figure 1H). Furthermore, calpain inhibitor III (20 μM to axons) prevented paclitaxel- induced degeneration, indicating axon fragmentation requires local calpain activation (Figure 1I). Together these results indicate that paclitaxel acts locally and directly on sensory neuron axons to initiate a degenerative process that culminates in calpain-dependent axonal fragmentation.

Paclitaxel impedes axonal localization of RNA transport granules and reduces *bclw* translation

Although anti-apoptotic Bcl2 family members are involved in developmental axon degeneration, it is uncertain whether Bcl2 family members are also critical for axon degeneration caused by injury or disease (Cosker et al., 2013; Courchesne et al., 2011; Nikolaev et al., 2009; Pazyra-Murphy et al., 2009; Schoenmann et al., 2010; Simon et al., 2016; Simon et al., 2012; Vohra et al., 2010). To determine if Bcl2 family members are implicated in paclitaxel-induced axon degeneration, we examined expression of the anti-apoptotic components Bclw (Bcl2l2), Bcl2, or $Bclx_L$ (Bcl2l1) after paclitaxel treatment. Since Bclw protein can be locally translated in axons (Cosker et al., 2013), we examined both mRNA and protein expression. Strikingly, paclitaxel treatment reduced both Bclw

mRNA and protein levels selectively in axons, and did not alter mRNA transcripts or protein expression in cell bodies (Figure 2A-2C). In contrast, paclitaxel treatment did not change Bcl2 and $Bclx_L$ mRNA or protein in axons or in cell bodies (Figure 2D-2I).

The RNA-binding protein SFPQ binds and transports *bclw* mRNA to the axon (Cosker et al., 2016), where it is locally translated into Bclw protein (Cosker et al., 2013). To determine if paclitaxel reduces axonal Bclw levels by hindering this sequence of events, we examined SFPQ expression after paclitaxel treatment. Paclitaxel caused a reduction in axonal SFPQ levels, without significantly altering SFPQ expression in the cell body compartment (Figure 3A and 3B), suggesting that paclitaxel impedes transport of SFPQ-containing RNA granules to axons. To ask if the decrease in SFPQ causes axon degeneration, we virally expressed a FLAG-tagged version of SFPQ (Figure S1) prior to paclitaxel treatment. Expression of exogenous SFPQ maintained axonal quantities of SFPQ and of Bclw (Figure 3C and 3D), and thereby prevented paclitaxel-induced axon degeneration (Figure 3E). As SFPQ is critical for intracellular transport and axonal translation of *bclw* mRNA (Cosker et al., 2016), we performed metabolic-labeling experiments to determine if paclitaxel specifically alters Bclw protein synthesis. The non-canonical amino acid azidohomoalanine (AHA) was used to label nascent proteins of DRG neurons in mass cultures that were treated with paclitaxel or a vehicle control for 3 or 9 hours. Paclitaxel treatment dramatically reduced synthesis of AHA-labeled Bclw. In contrast, paclitaxel treatment did not alter synthesis of AHA-labeled Bcl2 protein (Figure 3F and 3G). Thus, paclitaxel treatment of sensory neurons specifically impairs *bclw* translation. Together these data suggest paclitaxel, a microtubule stabilizing agent, diminishes axonal transport of SFPQ and its cargo, *bclw* mRNA, and thereby decreases Bclw synthesis.

Bclw prevents paclitaxel-induced degeneration

If paclitaxel-induced reduction of axonal Bclw leads to degeneration, then sustained Bclw levels in axons should prevent degeneration. Therefore, we asked if paclitaxel-induced degeneration can be prevented by recombinant Bclw, Bcl2, or $Bclx_L$ protein introduced selectively into axons of sensory neurons grown in compartmented cultures (Cosker et al., 2013). Bclw, introduced into axons, completely prevented paclitaxel-induced axon degeneration (Figure 4A, 4B, and S2). While both Bclw and $Bclx_L$ regulate developmental neurotrophin-dependent axon survival (Cosker et al., 2016; Cosker et al., 2013; Simon et al., 2016), we find that neither $Bclx_L$ nor Bcl2 prevents paclitaxel-induced degeneration even when protein is introduced directly into axons (Figure 4A, 4B, and S2). Furthermore, selective introduction of Bclw, Bcl2, or $Bclx_L$ protein into cell bodies did not inhibit paclitaxel-induced degeneration (Figure 4C). As calpain proteases are required for paclitaxel-induced degeneration, we analyzed the ability of Bclw to prevent calpain activation. We found that paclitaxel-induced calpain activation was selectively prevented by Bclw protein. Again, Bcl2 and $Bclx_L$ protein were not able to prevent calpain activation (Figure 4D). Together these data indicate that paclitaxel-induced reduction in Bclw expression promotes axon fragmentation, and identify Bclw as a specialized Bcl2 family member that functions locally in axons in a cascade that prevents calpain activation and degeneration.

The BH4 domain of Bclw is sufficient to prevent degeneration

Bclw, Bcl2, and $Bclx_L$ exhibit highly conserved structures with four characteristic Bcl2 homology (BH) domains. The BH4 domains mediate multiple anti-degenerative effects of these proteins (Barclay et al., 2015; Donnini et al., 2009; Hotchkiss et al., 2006; Mincheva-Tasheva et al., 2014; Monaco et al., 2015; Rong et al., 2009; Shimizu et al., 2000; Sugioka et al., 2003). While the BH4 domains of Bclw, Bcl2, and $Bclx_L$ exhibit a conserved alpha-helical structure, the nature and location of several of the protruding amino acid side chains differ in Bclw compared with Bcl2 or $Bclx_L$. To identify domain(s) of Bclw capable of preventing paclitaxel-induced degeneration, we generated a stabilized alpha-helix of Bcl2 domain (SAHB) modeled after the BH4 domain (aa 12-31) of Bclw (called Bclw BH4 $SAHB_A$), and SAHBs modeled after the BH4 domains of Bcl2 (aa 13-32) and $Bclx_L$ (aa 6-26; Figure 5A). SAHBs are alpha-helical hydrocarbon stapled peptides that are bioactive, protease-resistant, and cell-permeable (Barclay et al., 2015; Walensky and Bird, 2014). As described previously for Bcl2 BH4 $SAHB_A$ (Barclay et al., 2015), Bclw BH4 $SAHB_A$ inhibited Bax-mediated membrane poration of encapsulated liposomes in a dose-dependent manner, indicating this Bclw-mimetic has functional activity (Figure 5B). We transfected FITC-tagged BH4 peptides of Bclw, Bcl2, or $Bclx_L$ or a vehicle control into axons of compartmented cultures before treating axons with paclitaxel for 24 hours (Figure 5C). All three FITC-labeled peptides were detectable in axons and exhibited a punctate distribution. As observed with full-length Bclw, the Bclw BH4 $SAHB_A$ prevented paclitaxel-induced axon degeneration. In contrast, Bcl2 BH4 $SAHB_A$ and $Bclx_L$ BH4 $SAHB_A$ did not do so (Figure 5D). Importantly, equivalent intracellular bioactivity of these peptides in sensory neurons was confirmed using a neurotrophin-deprivation assay; transfection of Bclw BH4, Bcl2 BH4, or $Bclx_L$ BH4 SAHB peptides into cell bodies equally prevented apoptosis triggered by 24 hours of neurotrophin deprivation (Figure 5E). Together these results indicate that the BH4 domain of Bclw prevents paclitaxel-induced axon degeneration, a function that is not shared by the BH4 domains of Bcl2 and $Bclx_L$.

Bclw regulates IP_3R1 to prevent axon degeneration

The unexpectedly distinctive role of Bclw and its BH4 domain in preventing paclitaxel-induced degeneration suggests the Bclw BH4 domain may interact with different molecular targets than do Bcl2 and $Bclx_L$ in the axonal context. In addition to pro-apoptotic Bcl2 family members such as Bax, BH4 domains can also interact with inositol 1,4,5-trisphosphate receptors (IP_3Rs) such as IP_3R1 (Chang et al., 2014; Distelhorst and Bootman, 2011; Greenberg et al., 2014; Oakes et al., 2005; Rong et al., 2009). Notably, IP_3R1 has been implicated in injury-induced axon degeneration (Villegas et al., 2014). We examined co-precipitation of the biotinylated BH4 SAHB peptides with IP_3R1 from sensory neurons. Surprisingly, IP_3R1 from axons preferentially interacted with Bclw BH4 $SAHB_A$ (Figure 6A and 6B), while IP_3R1 from cell bodies interacted similarly with all three SAHBs (Figure 6C and 6D). Furthermore, biotinylated SAHBs for Bclw, Bcl2, and $Bclx_L$ all associated equally with the pro-apoptotic protein Bax, whether derived from axons or cell bodies. None of the SAHBs associated with a negative control protein in lysates from either axons or cell bodies (tyrosyl-tRNA synthetase, YARS, which is present at similar levels in both compartments; Figure 6A-6D). Together these results identify axonal IP_3R1 as a molecular partner that

selectively binds to the BH4 domain of Bclw and may be responsible for the specialized ability of Bclw to prevent axon degeneration.

IP_3Rs are resident endoplasmic reticulum (ER) calcium channels that control calcium release from intracellular stores. To determine whether paclitaxel alters IP_3R functionality, DRG neurons expressing the calcium indicator GCaMP6s were stimulated with ATP to trigger production of the IP_3R ligand IP_3 and thereby induce IP_3R-dependent calcium release from the ER. Paclitaxel treatment for 24 hours significantly reduced ATP-evoked IP_3R calcium release (Figure 6E), consistent with previous reports (Boehmerle et al., 2007). This finding suggests that paclitaxel either alters IP_3R activity or reduces intracellular calcium store levels. To distinguish between these possibilities, we examined intracellular calcium content by treating GCaMP6s-expressing cells with thapsigargin, a sarcoendoplasmic reticulum calcium ATPase (SERCA) inhibitor that induces calcium efflux from intracellular stores. Paclitaxel treatment did not alter thapsigargin-mediated calcium release (Figure 6F), indicating paclitaxel alters IP_3R activity rather than affecting the magnitude of intracellular calcium stores. Paclitaxel-induced changes in IP_3R activity have been attributed to paclitaxel-mediated degradation of the IP_3R modulatory protein neuronal calcium sensor 1 (NCS-1) (Boehmerle et al., 2007). However, we did not observe changes in the level of NCS-1 in response to paclitaxel treatment (Figure S3A). Changes in IP_3R1 phosphorylation state have also been shown to modulate IP_3R1 activity, as increased phosphorylation at serine 1756 (rat Ser1756; mouse Ser1755) correlates with increased sensitivity to IP_3 (Nakade et al., 1994; Oakes et al., 2005; Tang et al., 2003; Vanderheyden et al., 2009; Wagner et al., 2003; Wagner et al., 2004). Paclitaxel treatment for 24 hours lowered axonal Ser1756 phosphorylation, a finding consistent with evidence that paclitaxel reduces IP_3-gated ER calcium flux (Figure 6G). To address the importance of IP_3R1 activity for paclitaxel-induced axon degeneration, we used shRNA to reduce IP_3R1 in sensory neurons, and then assessed the response to paclitaxel. We find that knockdown of IP_3R1 (Figure S3B) prevents paclitaxel-induced degeneration (Figure 6H). Together these results indicate that paclitaxel treatment activates a conserved pathological axon degenerative cascade that is dependent on IP_3R1 and culminates in activation of calpain proteases.

To determine if Bclw and IP_3R1 function in the same pathway to regulate axon degeneration, neurons were infected with shRNAs targeting Bclw and/or IP_3R1 (Figure S3C). Acute knockdown of Bclw increased spontaneous axonal degeneration, and exacerbated paclitaxel-induced degeneration (Figure 6H), indicating that endogenous Bclw functions as a brake on a degenerative cascade activated by paclitaxel. Moreover, IP_3R1 knockdown completely prevented axon degeneration caused by Bclw knockdown or by paclitaxel, either individually or together (Figure 6H). Together these data indicate that Bclw functions upstream of IP_3R1 to prevent an axonal degenerative cascade that is triggered by paclitaxel.

The balance of anti-apoptotic and pro-apoptotic Bcl2 family members has been shown to regulate IP_3R1 phosphorylation and calcium dynamics. Bax, which binds to Bclw in axons (Figure 6A-6D), reduces IP_3R1 calcium leak and Ser1756 phosphorylation (Oakes et al., 2003; Oakes et al., 2005), and this functionality is distinct from the regulation of mitochondrial cytochrome *c* release. Since we observe a paclitaxel- induced decrease in

IP_3R1 phosphorylation at Ser1756 (Figure 6G), we asked if Bax is involved in axon degeneration caused by paclitaxel. Acute knockdown of Bax (Figure S3D) decreased paclitaxel-induced degeneration (Figure 6I). However, paclitaxel did not induce cytochrome *c* release from axonal mitochondria, as assessed by persistent cytochrome *c* colocalization with MitoTracker-labeled mitochondria after paclitaxel treatment (Figure S4A and S4B). As a positive control, we verified our capacity to visualize the decrease in mitochondrial cytochrome *c* immunostaining upon treatment with a pro-apoptotic kinase inhibitor K252A (Figure S4C). Taken together, our data suggest that Bax may be involved in paclitaxel-induced degeneration through action at the ER rather than its classical function in regulating mitochondrial outer membrane poration and cytochrome *c* release.

Loss of Bclw exacerbates paclitaxel-induced neuropathy *in vivo*

To examine the protective role of Bclw in paclitaxel-induced degeneration *in vivo*, we injected 2 month old *bclw*+/+ and *bclw*−/− mice with paclitaxel (4 mg/kg every other day for 8 days), a dose that mimics clinical protocols for paclitaxel therapy, or with a vehicle control. At this age, untreated *bclw*−/− mice exhibit normal epidermal innervation and sensory behavior (Courchesne et al., 2011). Consistent with prior studies in wildtype mice, both *bclw*+/+ and *bclw*−/− mice develop thermal hyperalgesia after paclitaxel treatment as measured by paw withdrawal in a 50°C hot-plate test (Figure 7A). However, the thermal pain sensitivity observed in *bclw*−/− mice after paclitaxel treatment was more severe than seen in age-matched *bclw*+/+ mice (Figure 7A). Both *bclw*+/+ and *bclw*−/− mice develop severe mechanical allodynia, as assessed by withdrawal responses to von Frey filaments (Figure 7B). In patients, paclitaxel causes a primarily sensory neuropathy with little to no motor symptoms (Gornstein and Schwarz, 2014); similarly, paclitaxel-treated mice have normal motor function as assessed by an accelerating RotaRod test (Figure S5). The gold standard for diagnosis of CIPN is reduced intraepidermal innervation. Therefore we examined intraepidermal nerve fibers of the hindpaw after paclitaxel or control treatments. Strikingly, we found that *bclw*−/− mice treated with paclitaxel exhibit a greater reduction in intraepidermal nerve fiber number in both thick (dermal papillae-containing; Figure 7C and 7D) and thin (non-dermal papillae containing; Figure 7E and 7F) skin than that detected in *bclw*+/+ mice. Together, these data demonstrate that Bclw functions to protect sensory axons from paclitaxel-induced degeneration *in vivo* as well as *in vitro*.

Discussion

In this study we use compartmented culture and *in vivo* systems to investigate the mechanisms underlying CIPN, and we demonstrate that paclitaxel acts directly on sensory axons to induce a Bclw- IP_3R1-dependent degenerative cascade. While previous studies highlighted the importance of the Bcl2 family in regulating caspase pathways and preventing developmental axon degeneration (Cosker et al., 2013; Cusack et al., 2013; Nikolaev et al., 2009; Schoenmann et al., 2010; Simon et al., 2012), here we identify a novel axon survival mechanism involving specific interactions between Bclw and axonal IP_3R1. Our results indicate that paclitaxel selectively reduces axonal Bclw levels by inhibiting transport of RNA granules containing the RNA-binding protein SFPQ and so impedes *bclw* mRNA axonal localization and translation. Therefore paclitaxel-induced degeneration can be

prevented by replenishing axonal stores of Bclw. Importantly, Bclw has a unique ability to protect axons from degeneration. Neither Bcl2 nor $Bclx_L$ prevents paclitaxel-induced degeneration, and paclitaxel does not alter the expression of these closely related Bcl2 homologs. Furthermore, the BH4 domain of Bclw, which selectively interacts with axonal IP_3R1, is sufficient for these specific protective effects. Together, these data indicate that paclitaxel causes neuropathy by reducing axonal Bclw, thus deregulating IP_3R1 signaling and permitting activation of IP_3R1-dependent degeneration.

The mechanism of action for paclitaxel is to prevent microtubule depolymerization and so enhance microtubule stability. Based on this activity, a prevalent hypothesis has been that paclitaxel reduces axonal transport of mitochondria (Gornstein and Schwarz, 2014; Shemesh and Spira, 2010). However, a recent study (Gornstein and Schwarz, 2017) demonstrates that paclitaxel causes retraction of sensory axons without reducing mitochondrial movement. We find that paclitaxel decreases axonal levels of SFPQ, an RNA-binding protein required for axonal trafficking of *bclw* mRNA, reduces *bclw* translation, and so results in decreased levels of Bclw protein in axons. These changes in axonal transport due to paclitaxel are functionally important in CIPN, as increased expression of SFPQ or of Bclw prevents paclitaxel-induced degeneration. Together, our data indicate that, rather than causing a global reduction in microtubule-based transport, paclitaxel selectively impinges on axonal transport of RNA granules (Bobylev et al., 2015) and thereby reduces translation of specific transcripts, including *bclw*, causing axonal degeneration.

Intriguingly, Bclw has a specialized ability to prevent paclitaxel-induced degeneration of sensory axons, a functionality not shared by the closely related Bcl2 or $Bclx_L$ proteins. This specialized role for Bclw is particularly surprising because $Bclx_L$, as well as Bclw, were recently shown to promote neurotrophin-dependent sensory axon survival (Cosker et al., 2013; Simon et al., 2016). During developmental axon degeneration, both Bclw and $Bclx_L$ prevent degeneration by binding and inhibiting the pro-apoptotic Bcl2 family members Bax and Puma (Simon et al., 2016). In contrast, in paclitaxel-induced axon degeneration, Bclw functions as a specialized upstream regulator of axonal IP_3R1. Thus, unlike closely related family members, Bclw has a distinctive ability to interact with IP_3R1 in axons, and exhibits a unique ability to protect axons from paclitaxel toxicity.

In addition to causing a reduction in axonal Bclw mRNA and protein, we find that paclitaxel alters sensory neuron calcium dynamics, a critical component in pathological axon degeneration (Figure 6E) (Benbow et al., 2012; Bobylev et al., 2015; Boehmerle et al., 2007; Chen et al., 2015; Mo et al., 2012; Yilmaz and Gold, 2015). While it is well accepted that a rise in axonal calcium is necessary for calpain activation and for axon degeneration, the source and trigger of this calcium increase are not clear. Early studies indicated a role for extracellular calcium influx (George et al., 1995; Schlaepfer and Bunge, 1973); however, more recent reports suggest that calcium from intracellular stores can also initiate calpain activation and axon degeneration following mechanical or toxic injury (Villegas et al., 2014). Our studies begin to delineate a pathway whereby paclitaxel deregulates IP_3R1 function and so alters intracellular calcium dynamics, ultimately resulting in elevated cytoplasmic calcium and calpain activation (Figure 8).

The decrease in IP_3-induced calcium release into the cytoplasm that we observed after 24 hours of paclitaxel treatment may reflect complex changes in location or timing of intracellular calcium dynamics. Our assay monitors overall IP_3-induced calcium release into the cytoplasm through IP_3R1, 2 and 3 (Figure 6E); the observed reduction in cytoplasmic calcium release may be associated with localized, increased calcium flux at mitochondrial associated membranes where IP_3R1 is clustered (Krols et al., 2016; Raturi and Simmen, 2013). Alternatively, early increases in calcium release from intracellular stores may be followed by a homeostatic decrease in IP_3-induced calcium release into the cytoplasm (Berridge et al., 2000), resulting in the altered calcium dynamics observed after 24 hours of paclitaxel treatment (Figure 6E). Together our data indicate that paclitaxel alters IP_3R function and intracellular calcium dynamics in a complex fashion, and that IP_3R1 is required for paclitaxel-induced degeneration.

Our findings suggest that axonal IP_3R1 interacts in a specialized manner with Bclw, and that these interactions are critical for the biological function of Bclw in promoting axonal survival. Although the native structures of the BH4 domains bound to their protein targets have not been fully defined, amino acid sequence and structure-based differences could underlie alternate binding and biological activities among Bcl2, $Bclx_L$, and Bclw. Three distinct sites on IP_3R1 have been identified as potential binding sites for the BH4 domain of Bcl2 family members (Bonneau et al., 2016; Rong et al., 2008; Schulman et al., 2013). Detailed analysis of the binding site(s) on IP_3R1 that are available within axons and of the molecular features that enable selective interactions with the Bclw BH4 SAHB may provide an approach for developing new therapies for CIPN.

We find that mice with genetic ablation of Bclw exhibit enhanced sensitivity to paclitaxel, suggesting that Bclw functions to limit paclitaxel-induced degeneration *in vivo*. Paclitaxel-induced thermal hyperalgesia and axon loss was enhanced in *bclw*−/− mice compared with their wild type littermates. Importantly, this enhanced response is observed in 2–3 month old *bclw*−/− mice that do not display the axon degeneration and thermal hypoalgesia observed in 4–8 month old *bclw*−/− mice (Courchesne et al., 2011). It is possible that axons of young *bclw*−/− mice are impaired prior to paclitaxel treatment, and that any mutation that causes neuropathy may enhance the effects of paclitaxel. However, paclitaxel does not simply accelerate the progressive neuropathy observed with increased age in *bclw*−/− mice, since enhanced response to thermal stimulation is observed with paclitaxel while decreased response to thermal stimulation was observed in older *bclw*−/− mice. Thus, while our studies suggest a protective role for Bclw in paclitaxel-induced degeneration, future studies will be required to determine the therapeutic relevance of restoring Bclw function to prevent paclitaxel-induced neuropathy in patients.

Based on our studies we propose a model in which paclitaxel attenuates axonal transport and translation of *bclw* in long axons and thereby removes the brakes on an axonal degenerative cascade (Figure 8). As paclitaxel enhances axon degeneration even in the absence of Bclw (Figure 6H and 7A-7F), paclitaxel may initiate additional pro-degenerative signals including changes in IP_3R1 phosphorylation state and activity. Strikingly, knockdown of IP_3R1 completely prevents paclitaxel-induced degeneration either in the presence or absence of Bclw, indicating that IP_3R1 functions downstream of Bclw to enable calpain-dependent

degeneration. Together, these studies suggest Bclw inhibits the pro-degenerative effects of IP_3R1 activity. As genetic ablation of the pro-degenerative molecule Sarm1 prevents paclitaxel-induced neuropathy (Turkiew et al., 2017), there is an intriguing possibility for intersection between the Sarm1-MAPK degenerative pathway (Yang et al., 2015) and the SFPQ-Bclw-IP_3R1 cascade identified here.

Our studies further reveal that Bax contributes to paclitaxel-induced degeneration. Bax is most well-known for its function at the mitochondria, where it mediates mitochondrial membrane poration to induce cytochrome *c* release and activation of the caspase cascade. However, paclitaxel treatment does not induce cytochrome *c* release, suggesting Bax may play a different role in paclitaxel-induced degeneration. Notably, Bax is also present in the ER, where it alters IP_3R1 phosphorylation state and modulates ER calcium dynamics (Oakes et al., 2003; Scorrano et al., 2003; Zong et al., 2003). These changes in calcium dynamics may represent the critical function of Bax in the context of CIPN. Although $Bclx_L$ and Bcl2 full length proteins or BH4 SAHB domains all bind Bax and prevent Bax-mediated apoptosis (Figure 5E and 6A-6D) (Barclay et al., 2015; Petros et al., 2004), they do not prevent paclitaxel-induced degeneration. Thus, compounds such as Bclw BH4 SAHBs that mimic Bclw interactions with IP_3R1 without impinging on the ability of Bax to initiate axonal cytochrome *c* release may provide a promising therapeutic strategy for CIPN.

Despite the prevalence and morbidity of CIPN, at present there are no methods to prevent or reverse this disorder (Brewer et al., 2016; Cavaletti and Marmiroli, 2010; Pachman et al., 2011). Current treatment options therefore are to reduce or discontinue chemotherapy, and to offer non-specific symptomatic pain relief. In rodent models, systemic calpain inhibition reduces the neurotoxic effects of paclitaxel *in vivo* (Wang et al., 2004), and calcium chelation reduces paclitaxel-induced neuropathic pain (Siau and Bennett, 2006). Here we show that a stabilized alpha-helix of the Bclw BH4 domain binds to IP_3R1 and prevents paclitaxel-induced calpain activation and degeneration, indicating this designer peptide provides a promising template for drugs that can prevent CIPN. IP_3R1 is also required for axon degeneration induced by other chemotherapeutic agents (Villegas et al., 2014), and alterations in calcium are implicated in axon degeneration due to diverse causes (Coleman, 2005). Therefore, reduction in Bclw and consequent activation of IP_3R1-dependent axonal fragmentation may represent a conserved mechanism for many neurodegenerative syndromes.

STAR Methods

CONTACT FOR REAGENT AND RESOURCE SHARING

Further information and requests for resources and reagents should be directed to and will be fulfilled by the Lead Contact, Rosalind Segal (rosalind_segal@dfci.harvard.edu). AAV9 viral vectors were obtained from the Penn Vector Core and require an MTA.

EXPERIMENTAL MODEL AND SUBJECT DETAILS

Mouse lines and animal care—All experimental procedures were conducted in accordance with the National Institutes of Health guidelines and were approved by the

Dana-Farber Cancer Institutional Animal Care and Use Committee. Timed pregnant Sprague-Dawley rats were purchased from Charles River. *bclw−/−* mice were a generous gift from Grant MacGregor (University of California, Irvine, CA; (Ross et al., 1998). Genotyping for the wild-type *bclw* gene and/or lacZ gene were performed by Transnetyx using the Bclw targeting sequence GCTCTGAACCTCCCCATGACTTAAATCCGTTGCTCTTTCT-TGGCCCTGCCCAGTGCCTCTGAGCATTTCACCTATCTCAGGAGC and the lacZ sequence CGATCGTAATCACCCGAGTGTGATCATCTGGTCGCTGGGGAATGAGTCAGGCCAC G-G. *bclw−/−* mice were maintained on a C57BL/6JEiJ background (Navarro et al., 2012).

Cell culture—Compartmented chamber (Campenot) cultures were prepared as described previously (Fenstermacher et al., 2015) with modifications. Briefly, DRGs from embryonic day 15 (E15) rats of either sex were dissected and trypsinized. DRG neurons (1.2×10^5 cells) were plated in the center compartment of a Teflon divider (Camp10, Tyler Research; Campenot, 1982) affixed to a p35 culture dish coated with growth factor reduced Matrigel basement membrane (1:45 in DMEM; BD Biosciences). Cultures were maintained in media consisting of Neurobasal (Invitrogen) with 2% B27 supplement (Invitrogen), 1% penicillin-streptomycin, 1% GlutaMAX (Life Technologies), 0.08% glucose, and 0.3 μM cytosine arabinoside (AraC) at 37°C, 7.5% CO^2; BDNF + NGF (PeproTech) were added to the cell body compartment at a concentration of 10 ng/mL and to the axon compartment at a concentration of 100 ng/mL for 2d. On day 3, media was replaced and the AraC was omitted. On day 5 neurotrophins were removed from the cell body compartment and reduced to 1 ng/mL in the axon compartments for 3–5 days. For paclitaxel treatment experiments, 30 nM paclitaxel (Sigma-Aldrich) or vehicle control (0.1% DMSO) was added to either cell body or distal axon compartments on day 7 for 24 hours. For calpain inhibition experiments, 20 μM calpain inhibitor III (VWR) and paclitaxel were added simultaneously to distal axon compartments.

Microfluidic chambers cultures were prepared as described previously (Fenstermacher et al., 2015), with modifications. Briefly, 3×10^4 E15 DRG neurons (4 μL volume) were plated into one channel of a microfluidic device (Xona Microfluidics, SND450) affixed to a PDL/laminin-coated cover glass (Fisherbrand Microscope Cover Glass; 24×40–1.5). Cells were plated in Neurobasal media (described above) with 0.3 μM AraC; 50 ng/mL NGF + BDNF was added to cell body wells, and 100 ng/mL was added to axon wells. On day 2, cell body neurotrophins were reduced to 10 ng/mL. On day 4 or 5, cell body neurotrophins were reduced to 1 ng/mL and axon neurotrophins were reduced to 10 ng/mL, and cultures were maintained for 1–3 more days. For paclitaxel treatment experiments, 60 nM paclitaxel or vehicle control was added to the distal axon compartment for 24–48 hours to observe changes in axons. Non-compartmented, mass cultures consisting of 3×10^5 E15 DRG neurons were grown on Matrigel-coated p35 culture dishes in neurotrophin-enriched (100 ng/mL NGF + BDNF) media with 0.3 μg/mL AraC. On day 3, neurotrophins were reduced to 10 ng/mL) and cultures maintained for 3–6 more days. To observe changes in calcium signaling or translation levels, 600 nM paclitaxel was added globally to cultured neurons. Higher doses are required for cultures that contain cell bodies and so include greater cellular

material, only a small portion of which is axonal. 600 nM paclitaxel causes degeneration and significantly increases calpain activity in mass cultures (Figure 1H), but calpain activation can still be prevented by expression of the Bclw BH4 SAHB$_A$ (Figure 4D), suggesting the same Bclw-calpain pathway is engaged as with 30 nM paclitaxel.

METHODS DETAILS

Axonal degeneration assay—Compartmented chamber cultures were fixed at room temperature with 4% PFA diluted 1:2 in media for 10 min, then undiluted 4% PFA for an additional 20 min. Cultures were permeabilized with 0.1% Triton X-100 for 10 minutes, blocked in 3% BSA and 0.1% Triton X-100 for 1 hour at room temperature, and incubated with mouse anti-Tuj1 (1:400; clone Tuj1; Covance) overnight at 4°C. Cultures were then incubated with goat anti-mouse AlexaFluor (1:1000; Invitrogen) for 1 hour at room temperature and counterstained with DAPI. Images of distal axon tips were obtained using a 40× air objective, and axonal degeneration was quantified as a degeneration index, as previously described (Cosker et al., 2013; Sasaki et al., 2009). Apoptosis analysis was carried out on the same cultures by taking images in the cell body compartment and counting total and condensed nuclei in NIH ImageJ software by an observer blind to condition.

Mitochondrial membrane potential measurements—E15 DRG neurons grown in microfluidic cultures were treated with 60 nM paclitaxel to the axonal compartment for 48 hours, then labeled using Tetramethylrhodamine ethyl ester (TMRE) (Invitrogen). TMRE was applied (10 nM) for 20 min at 37°C, then cells were rinsed with phenol-free media and imaged live using a 60× oil 1.4NA objective. Fluorescence intensity of axonal mitochondria was measured by dividing the fluorescence intensity of each mitochondria (Fm) by the background fluorescence intensity of a nearby cytoplasmic region (Fc). Fluorescence intensity was measured using NIH ImageJ software by an observer blind to condition.

Mitochondrial length measurements—E15 DRG neurons grown in microfluidic cultures were treated with 60 nM paclitaxel to the axonal compartment for 48 hours, and fixed at room temperature with 4% PFA diluted 1:2 in media for 10 min, then undiluted 4% PFA for an additional 10 min. Cultures were permeabilized and blocked as above and incubated overnight at 4°C with the following antibodies: anti-Tomm20 (1:300; Abcam), and anti-Tuj1. Cultures were then stained with AlexaFluor antibodies and counterstained with DAPI as above. Images were acquired throughout the axon compartment using a 60× 1.4NA oil objective, and Tomm20 mitochondrial length was measured manually using NIH ImageJ by an experimenter blind to condition. 1078 (vehicle) and 1049 (paclitaxel) axonal mitochondria were measured across three independent experiments.

Quantitative reverse transcription-PCR—RNA was extracted from DRG neurons in compartmented cultures using TRIzol (Invitrogen) according to manufacturer's protocol. Reverse transcription (RT) was performed using the cDNA archive kit (Applied Biosystems) according to the manufacturer's protocol, and quantitative real-time RT-PCR was performed using Taqman Gene expression assays (Applied Biosystems) to analyze expression of *bclw* (Rn00821025_g1), *bcl2* (Rn99999125_m1), and *bclx$_L$* (Rn00580568_g1). Data were

normalized to *gapdh* (glyceraldehyde-3-phosphate dehydrogenase; Applied Biosystems) for each sample.

Western blot—For analysis of Bcl2 family proteins, SFPQ, and IP_3R1 phosphorylation, cell bodies and axons of E15 DRGs in compartmented cultures were lysed in nonionic detergent, lysates were separated by 4–12% Bis-Tris or 3–8% Tris-Acetate SDS-Page (Thermo Fisher Scientific), and probed with the following antibodies: anti- Bclw (1:1000; clone 31H4; Cell Signaling Technology), anti-Bcl2 (1:1000; Abcam), anti-$Bclx_L$ (1:1000; Cell Signaling Technology), anti-GAPDH (1:2000; clone 14C10; Cell Signaling Technology), anti-SFPQ (1:1000; clone 6D7; Sigma-Aldrich), anti-Phospho-IP_3R1 Ser1756 (1:500; clone D10E3; Cell Signaling), and anti- IP_3R1 (1:1000; Thermo Scientific). Bands were visualized with secondary antibodies conjugated to HRP (1:10,000; Bio-Rad) and SuperSignal chemiluminescent substrate signal. Using NIH ImageJ software, protein levels were quantified and levels of protein were normalized to GAPDH.

Lentiviral transduction—For viral overexpression or knockdown studies, 50 μL lentivirus was added to cell bodies of compartmented cultures for 24 hours, then virus was removed, media containing puromycin (1 μg/mL; Sigma-Aldrich) was added, and cultures were allowed to grow for 5 days prior to paclitaxel treatment. For SFPQ overexpression, a lentivirus construct expressing the FLAG-tagged coding sequence of human SFPQ was generated. An RFP-expressing virus was used as the control. For shRNA lentiviral knockdown, lentiviral constructs expressing shRNAs targeting rat IP_3R1 (TRCN0000321161; Sigma-Aldrich), Bclw (TRCN0000321174; Sigma-Aldrich), or Bax (TRCN0000273039; Sigma-Aldrich) were generated, and knockdown efficacy was verified by reduction of protein levels in mass cultured DRGs (Figure S3B-S3D). An RFP-targeting shRNA was used as the control shRNA. This approach decreases expression of the targeted proteins throughout the whole cell.

Metabolic labeling of nascent protein synthesis—DIV5 DRG neurons grown in mass culture were starved at 5 days *in vitro* (DIV) for one hour in Methionine/Cysteine/Glutamine triple dropout DMEM supplied with 1% Glutamax, 1% penicillin- streptomycin, 10ng/ml NGF+BDNF. 200 μM L-Cysteine and 200 μM Click-IT AHA (L-Azidohomoalanine; Life Technologies C10102) were then added to the medium together with 600 nM Paclitaxel or DMSO vehicle. Cells were then harvested at 3 or 9 h after paclitaxel or vehicle addition. Cells were lysed and sonicated in AHA lysis buffer (20mM TRIS-Cl pH7.4, 140mM NaCl, 10% Glycerol, 1% SDS, protease inhibitor cocktail). Protein concentration was determined with Pierce BCA protein assay kit (Thermo Scientific). Click-IT reaction was performed using Click-IT protein reaction buffer kit (Invitrogen C10276) following manufacturer's instruction. Briefly, 200 μg protein for each condition was mixed with 20 μM Biotin Alkyne (Life Technologies B10185), 10 μl Copper Sulfate Solution, 10 μl Additive I and 20 μl Additive II in the reaction buffer for 20 min. The excess biotin was then removed using Bio-Spin(R) P-6 Gel Columns (BioRad 7326227). 10% of each reaction by volume was kept as input and the rest was incubated for 2 h with 50 μl Dynabeads Myone Streptavidin T1 (Invitrogen 65601) pre-blocked with 1% BSA in PBS with 0.1% Tween-20.

The Streptavidin T1 beads were then washed with PBS with 0.1% Tween-20 for three times, followed by elution in SDS loading buffer for 5 min at 95°C.

Stapled peptide synthesis—Stapled peptides were synthesized, derivatized at the N-terminus with FITC-bALA or biotin-bAla, purified by LC-MS to > 95% purity, and quantified by amino acid analysis according to our established methods (Barclay et al., 2015; Bird et al., 2008). Lyophilized SAHBs were reconstituted in 100% DMSO and diluted into aqueous buffers for experimentation. The following peptide sequences were used, where X = pentenyl alanine and where B = norleucine, replacing a cysteine:

Bclw BH4 SAHB$_A$	ALVADFVGYKLRXKGYXBGA
Bcl2 BH4 SAHB$_A$	EIVBKYIHYKLSXRGYXWDA
Bclx$_L$ BH4 SAHB$_A$	RELVVDFLSYKLSXKGYXWSQ
BIM BH3 SAHB$_{A2}$	EIWIAQELRXIGDXFNAYYA

Liposomal release assay—Large unilamellar vesicles with lipid composition resembling the mitochondrial outer membrane were generated and entrapped with ANTS and DPX as described (Leshchiner et al., 2013; Lovell et al., 2008). Recombinant Bax was generated in BL-21 DE3 *E. Coli* and then purified by chitin affinity and size exclusion chromatography as described (Edwards et al., 2013; Gavathiotis et al., 2008). For measurement of BIM BH3 SAHB$_{A2}$-induced activation of BAX, recombinant, full-length BAX protein, BIM BH3 SAHB$_{A2}$ (aa 145-164), and Bclw BH4 SAHB$_A$ were added at the indicated concentrations to liposomes (5 μl) to a final volume of 30 μl in 384-well plate format. ANTS dequenching due to DPX dissociation (F) upon liposomal release was measured over a period of 7200 seconds with a Tecan M1000 plate reader (excitation and emission wavelengths of 355 and 520 nm, respectively). Plates were re-read following lysis with 1% Triton X-100 to determine maximal release (F100). Percent ANTS/DPX release was calculated according to the equation [(F - F0)/(F100 - F0)] where F0 is the baseline fluorescence at time zero and F is the recorded fluorescence for a given experimental time point.

Protein and peptide introduction—Recombinant His-tagged Bclw, Bcl2, and Bclx$_L$ proteins (R&D Systems) or control β-Galactosidase protein were introduced into cell bodies or axons of compartmented chamber cultures as in Cosker et al., 2016. Briefly, 1 μg/μL protein was introduced into cultures using 2 μL Chariot reagent (Active Motif). FITC-SAHB peptides (Bclw BH4 SAHB$_A$, Bcl2 BH4 SAHB$_A$, and Bclx$_L$ BH4 SAHB$_A$; stock solutions 1 mM in DMSO) were introduced into cell bodies or axons using 350 ng peptide and 2 μL of Chariot reagent diluted 1:10 in water. Control was no peptide with 2 μL of 1:10 diluted Chariot. To confirm expression of His-tagged proteins, cell bodies and axons were washed and then lysed in nonionic detergent, and protein lysates were separated by 4–12% Bis-Tris (Thermo Fisher Scientific) and probed with the following antibodies: anti-His (1:1000; Novagen) and anti-pan-Actin (1:1000; Cell Signaling Technology). To confirm peptide uptake, cultures were processed for axonal degeneration assay as above, and FITC

immunofluorescence was examined with a 40× air objective. Paclitaxel was added to cultures 1 hour after protein or peptide transfection.

Neurotrophin-deprivation—FITC-SAHBs (Bclw, Bcl2, and $Bclx_L$ or no peptide control; 350ng) were transfected into the cell body compartment of compartmented cultures using the Chariot system as described above. One hour later, both cell body and axon compartments were changed into media without NGF + BDNF for 24 hours. A non-transfected control culture was maintained in 100 ng/mL NGF + BDNF media. Cultures were fixed and incubated with DAPI (1:1000). Images were taken with a 40× air objective, and an observer blind to condition counted the number of total and condensed nuclei using NIH ImageJ software.

Calpain protease activity luminescence assay—For paclitaxel dose response assay, DRG neurons in mass cultures were treated with paclitaxel (30 nM, 600 nM, or 1.2 μM for 48 h), calcium chloride (3 mM for 24 h), or vehicle control (0.1% DMSO for 48 h). For Bcl2 family rescue assay, DRG neurons in mass cultures were transfected using the Chariot system as above with His-tagged Bclw, Bcl2, and $Bclx_L$ proteins or untransfected control, then treated for 24 h with 600 nM paclitaxel or vehicle control. Cultures were harvested in 1× Passive Lysis Buffer (Promega). Lysate was spun 10,000×g for 5 minutes at 4°C, and 50 μL supernatant was combined with 50 μL Calpain-Glo Reagent (Promega) in a 96 well plate. Plate was shaken briefly and incubated 40 minutes in the dark; luminescence intensity was measured with a microplate reader and normalized to protein concentration.

Biotinylated SAHB pulldowns—E15 DRG neurons were grown in compartmented chamber cultures for 7–8 days, and cell bodies and axons were separately harvested in lysis buffer containing 1% CHAPS detergent, 150 mM NaCl, 50 mM Tris pH 7.4, 1 mM DTT, 1 mM NaF, 0.1 mM PMSF, 0.1 mM Na_3VO_3, and EDTA-free cOmplete Mini protease inhibitor cocktail (Sigma-Aldrich). Lysate was pre-cleared 2 hours at 4°C with High Capacity Neutravidin Agarose Beads (1:20 in lysate; Thermo Scientific). For each pulldown, 200–600 μg of precleared lysate was incubated overnight at 4°C with biotin alone or with biotinylated-BH4 SAHB peptides of Bclw, Bcl2, or $Bclx_L$ to a final peptide or biotin concentration of 20 μM. The next day, Neutravidin beads were added (1:14) to lysate for 2 h at 4°C. Lysate was removed, beads were washed on ice with cold PBS + protease inhibitor cocktail, and sample was eluted by boiling for 5 minutes in non- ionic lysis buffer, sample buffer, and reducing agent. Protein was resolved with either 4–12% Bis-Tris SDS-page (Bax, YARS, IP_3R1) or 3–8% Tris-Acetate SDS-page (YARS, IP_3R1) and probed with the following antibodies: anti-Bax (1:1000; Cell Signaling), anti-YARS (1:500; tyrosyl tRNA synthetase; clone EPR9927; Abcam), and anti-IP_3R1 (1:1000; Thermo Scientific). YARS was used as a negative control as this protein is present at similar levels in axons and cell bodies. A 10% input lane from the original cell body or axon lysate was run alongside pulldown lysate. Band intensity was quantified as described above, and each pulldown intensity was normalized to the input intensity.

Calcium imaging—E15 DRG neurons in microfluidic devices were infected on DIV0 with AAV9-GCaMP6s (AAV9.CAG.GCaMP6s.WPRE.SV40) and AAV9-mCherry

(AAV9.CB7.CI.mCherry.WPRE.rBG) for 24 hours (Penn Vector Core). After 4–5 days, 600 nM paclitaxel or vehicle control (0.1% DMSO) were added to both cell body and axon compartments for 24 hours. Cultures were incubated 15 minutes (37°C, 7.5% CO^2) in calcium-free media (130 mM NaCl, 4.7 mM KCl, 2.3 mM $MgSO_4$, 1.2 mM KH_2PO_4, 10 mM EGTA, 20 mM HEPES pH 7.3, 5 mM Glucose), then imaged with a Nikon Ti-E at 37°C (60× oil 1.4NA objective) while cells bodies were stimulated with 200 μM ATP (Sigma-Aldrich) or 5 μM thapsigargin (Thermo Fisher Scientific) in calcium-free media. For two fields of view, GCaMP6s and mCherry channels were acquired every 5 seconds for 60 seconds, then every 20 seconds for 440 seconds. ATP or thapsigargin was added after 15 seconds of baseline measurements. Images were analyzed using NIH ImageJ software. For each individual cell at each timepoint, a mask was generated from mCherry channel; GCaMP6s and mCherry fluorescence intensities were measured; and background fluorescence was subtracted. The change in fluorescence (ΔF/F) was calculated per cell according to the equation [(F - F0)/F0)] where F0 is the average baseline fluorescence at time 0–15 seconds and F is the recorded fluorescence for a given experimental time point. For ATP stimulation, 119 (paclitaxel) and 156 (vehicle) neuronal cell bodies were measured across 3 independent experiments with 3 cultures per experiment. For thapsigargin stimulation, 196 (paclitaxel) and 233 (vehicle) neuronal cell bodies were measured across 3 independent experiments with 3 cultures per experiment.

Cytochrome *c* immunostaining—E15 DRG neurons grown in microfluidic cultures were treated with 60 nM paclitaxel to the axonal compartment for 48 hours and mitochondria were labeled with 200 nM MitoTracker Red CMX ROS (Thermo Fisher Scientific) in media for 15 minutes at 37°C, washed with HBSS, and incubated 1 minute with an ice cold methanol wash before fixation with 4% PFA for 15 minutes. Cultures were stained as above with anti-cytochrome *c* (1:100; clone 6H2.B4; Thermo Fisher Scientific). Images were acquired throughout the axon compartment. Colocalization was quantified in ImageJ by doing a background subtraction and using the JACoP plugin (Bolte and Cordelieres, 2006) to calculate the thresholded Mander's overlap coefficient (tMOC) representing the fraction of cytochrome *c* overlapping MitoTracker-labeled mitochondria. An intensity threshold for each channel was set manually for each experiment based on a control image. 15 (paclitaxel) and 14 (vehicle) images were measured across 3 independent experiments. As a positive control for induction of cytochrome *c* release, cultures were treated globally with 200 nM K252a in media lacking neurotrophins for 48 hours, and a reduction in tMOC was confirmed.

Paclitaxel treatment and behavioral testing—2 month old age-matched *bclw*−/− and *bclw*+/+ mice (17–30 g) of both sexes were injected intraperitoneally (IP) with 4 mg/kg paclitaxel (Bristol-Myers Squibb) every other day for 8 days (4 total injections). Equivalent ratio of males to females was used in each group and sex did not alter the results. Paclitaxel was prepared as 1 part 6 mg/mL paclitaxel stock solution diluted in vehicle (1:1 v/v Cremophor EL [EMD Millipore] and dehydrated ethanol) and 2 parts sterile saline and injected at 10 μL/g. Control mice were injected with 1 part vehicle and 2 parts saline. At 4–6 months of age *bclw*−/− mice have altered noxious thermosensation; however 2–3 month old *bclw*−/− mice exhibit normal motor function and noxious sensation (Courchesne et al.,

2011). For three days prior to the baseline testing, mice were weighed, trained on an automated RotaRod apparatus (4 rpm for 1 minute without falling), and habituated in von Frey cages. The next two days, baseline behavioral performance was assessed and averaged. The first paclitaxel injection was given three days later, and mice were weighed and behaviorally tested 10 days after the final injection. Noxious mechanosensation threshold was assayed as described previously (Courchesne et al., 2011) using von Frey filaments (0.008–1.4g). Withdrawal threshold was determined to be the applied force at which the animal withdrew the stimulated paw on at least 2 of 10 applications. Noxious thermal sensation threshold was assayed as described previously (Courchesne et al., 2011) using a 50°C hotplate and measuring latency to withdraw the hindpaw. To assay motor function, mice were placed on the RotaRod with a ramp of 4–40 rpm and 0.4 rpm/sec acceleration, and latency to fall was measured. Mouse behavior was assessed by an experimenter blind to genotype and condition.

Epidermal footpad innervation—Footpad tissue from hindpaws of *bclw−/−* and *bclw +/+* mice was harvested, fixed, and sectioned as done previously (Cosker et al., 2013). Briefly, mice were euthanized with isoflurane 11 days after final paclitaxel injection and footpad tissue was removed and divided into thick (dermal papillae containing) and thin (non-dermal papillae containing) skin. Footpads were fixed in Zamboni's fixative overnight at 4°C, cryopreserved in 30% sucrose overnight at 4°C, frozen, and sectioned into 30 μm floating sections. Sections were blocked in 10% normal goat serum with 0.1% Triton X-100 in PBS 1 hour at room temperature and incubated with anti-Tuj1 (1:300; Covance) overnight at 4°C. Sections were then incubated with goat anti-mouse AlexaFluor 488 (1:200; Invitrogen) and DAPI (1:1000) for 2 hours at room temperature and mounted on gelatin-coated slides. Epidermal images were acquired on a Nikon Ni-E C2 confocal with a 40× 1.3NA oil objective as 30–35 μm z-stacks (1 μm step size) and converted into a maximum intensity projection image. Intraepidermal nerve fiber density was determined to be the number of Tuj1-positive fibers penetrating ≥10 μm into the epidermis, normalized to the measured epidermal length (225–450 μm per image) and displayed as number of Tuj1-positive fibers per 225 μm. Images were acquired and quantified in NIH ImageJ by an experimenter blind to genotype and condition.

QUANTIFICATION AND STATISTICAL ANALYSIS

Data are expressed as mean + SEM or ± SEM. To assess statistical significance, data were analyzed by unpaired two-tailed Student's *t* test. Calcium imaging experiments were analyzed by two-way ANOVA with *post hoc* Bonferroni correction. For all other multiple comparisons, data were analyzed by one-way ANOVA with *post hoc* Bonferroni or Dunnett correction unless otherwise indicated. Significance was placed at $p<0.05$ unless otherwise indicated. Statistical analysis was done using Microsoft Excel and GraphPad Prism.

Supplementary Material

Refer to Web version on PubMed Central for supplementary material.

Acknowledgments

We thank Grant MacGregor (University of California, Irvine, CA) for providing *bcl2l2* mice. We thank the GENIE Program and the Janelia Farm Research Campus, particularly Vivek Jayaraman, Rex A. Kerr., Douglas S. Kim, Loren L. Looger, and Karel Svoboda (GENIE Project, Janelia Farm Research Campus, HHMI) for distribution of the GCaMP6s materials. We thank Emily Chadwick for assistance with *bcl2l2* mice; Bernardo Sabatini and Lisa Cameron for advice on calcium imaging; Katharina Cosker for helpful discussions; and the Segal lab for helpful comments on the manuscript. This work was supported by the National Institutes of Health Grants R01 NS050674 and R01 CA205255 to R.A.S., R50 CA211399 to G.H.B., and R35 CA197583 to L.D.W., the Barr Weaver Award to R.A.S., the Harvard/MIT Joint Research Grant to R.A.S., and the Edward R. and Anne G. Lefler Center Predoctoral Fellowship to S.E.P.-R.

References

Anderson MA, Deng J, Seymour JF, Tam C, Kim SY, Fein J, Yu L, Brown JR, Westerman D, Si EG, et al. The BCL2 selective inhibitor venetoclax induces rapid onset apoptosis of CLL cells in patients via a TP53-independent mechanism. Blood. 2016; 127:3215–3224. [PubMed: 27069256]

Barclay LA, Wales TE, Garner TP, Wachter F, Lee S, Guerra RM, Stewart ML, Braun CR, Bird GH, Gavathiotis E, et al. Inhibition of Pro-apoptotic BAX by a noncanonical interaction mechanism. Molecular cell. 2015; 57:873–886. [PubMed: 25684204]

Barrientos S, Martinez N, Yoo S, Jara J, Zamorano S, Hetz C, Twiss J, Alvarez J, Court F. Axonal degeneration is mediated by the mitochondrial permeability transition pore. The Journal of neuroscience : the official journal of the Society for Neuroscience. 2011; 31:966–978. [PubMed: 21248121]

Benbow JH, Mann T, Keeler C, Fan C, Hodsdon ME, Lolis E, DeGray B, Ehrlich BE. Inhibition of paclitaxel-induced decreases in calcium signaling. The Journal of biological chemistry. 2012; 287:37907–37916. [PubMed: 22988235]

Berridge MJ, Lipp P, Bootman MD. The versatility and universality of calcium signalling. Nat Rev Mol Cell Biol. 2000; 1:11–21. [PubMed: 11413485]

Bird GH, Bernal F, Pitter K, Walensky LD. Synthesis and biophysical characterization of stabilized alpha-helices of BCL-2 domains. Methods Enzymol. 2008; 446:369–386. [PubMed: 18603134]

Bobylev I, Joshi A, Barham M, Ritter C, Neiss WF, Höke A, Lehmann HC. Paclitaxel inhibits mRNA transport in axons. Neurobiology of disease. 2015

Bodur C, Basaga H. Bcl-2 inhibitors: emerging drugs in cancer therapy. Current medicinal chemistry. 2012; 19:1804–1820. [PubMed: 22414090]

Boehmerle W, Zhang K, Sivula M, Heidrich FM, Lee Y, Jordt S-EE, Ehrlich BE. Chronic exposure to paclitaxel diminishes phosphoinositide signaling by calpain-mediated neuronal calcium sensor-1 degradation. Proc Natl Acad Sci U S A. 2007; 104:11103–11108. [PubMed: 17581879]

Bolte S, Cordelieres FP. A guided tour into subcellular colocalization analysis in light microscopy. J Microsc. 2006; 224:213–232. [PubMed: 17210054]

Bonneau B, Ando H, Kawaai K, Hirose M, Takahashi-Iwanaga H, Mikoshiba K. IRBIT controls apoptosis by interacting with the Bcl-2 homolog, Bcl2l10, and by promoting ER-mitochondria contact. Elife. 2016; 5:e19896. [PubMed: 27995898]

Brewer JR, Morrison G, Dolan ME, Fleming GF. Chemotherapy-induced peripheral neuropathy: Current status and progress. Gynecol Oncol. 2016; 140:176–183. [PubMed: 26556766]

Cavaletti G, Marmiroli P. Chemotherapy-induced peripheral neurotoxicity. Nat Rev Neurol. 2010; 6:657–666. [PubMed: 21060341]

Chang MJ, Zhong F, Lavik AR, Parys JB, Berridge MJ, Distelhorst CW. Feedback regulation mediated by Bcl-2 and DARPP-32 regulates inositol 1,4,5-trisphosphate receptor phosphorylation and promotes cell survival. Proc Natl Acad Sci U S A. 2014; 111:1186–1191. [PubMed: 24395794]

Chen L-HH, Sun Y-TT, Chen Y-FF, Lee M-YY, Chang L-YY, Chang J-YY, Shen M-RR. Integrating Image-Based High-Content Screening with Mouse Models Identifies 5-Hydroxydecanoate as a Neuroprotective Drug for Paclitaxel-Induced Neuropathy. Molecular cancer therapeutics. 2015; 14:2206–2214. [PubMed: 26294744]

Chipuk JE, Moldoveanu T, Llambi F, Parsons MJ, Green DR. The BCL-2 family reunion. Molecular cell. 2010; 37:299–310. [PubMed: 20159550]

Coleman M. Axon degeneration mechanisms: commonality amid diversity. Nat Rev Neurosci. 2005:6.

Cosker KE, Fenstermacher SJ, Pazyra-Murphy MF, Elliott HL, Segal RA. The RNA-binding protein SFPQ orchestrates an RNA regulon to promote axon viability. Nat Neurosci. 2016; 19:690–696. [PubMed: 27019013]

Cosker KE, Pazyra-Murphy MF, Fenstermacher SJ, Segal RA. Target-derived neurotrophins coordinate transcription and transport of bclw to prevent axonal degeneration. The Journal of neuroscience : the official journal of the Society for Neuroscience. 2013; 33:5195–5207. [PubMed: 23516285]

Courchesne SL, Karch C, Pazyra-Murphy MF, Segal RA. Sensory neuropathy attributable to loss of Bcl-w. The Journal of neuroscience : the official journal of the Society for Neuroscience. 2011; 31:1624–1634. [PubMed: 21289171]

Cusack CL, Swahari V, Hampton Henley W, Michael Ramsey J, Deshmukh M. Distinct pathways mediate axon degeneration during apoptosis and axon-specific pruning. Nature communications. 2013; 4:1876.

Distelhorst CW, Bootman MD. Bcl-2 interaction with the inositol 1,4,5-trisphosphate receptor: role in Ca(2+) signaling and disease. Cell Calcium. 2011; 50:234–241. [PubMed: 21628070]

Donnini S, Solito R, Monti M, Balduini W, Carloni S, Cimino M, Bampton ET, Pinon LG, Nicotera P, Thorpe PE, Ziche M. Prevention of ischemic brain injury by treatment with the membrane penetrating apoptosis inhibitor, TAT-BH4. Cell Cycle. 2009; 8:1271–1278. [PubMed: 19305142]

Edwards AL, Gavathiotis E, LaBelle JL, Braun CR, Opoku-Nsiah KA, Bird GH, Walensky LD. Multimodal interaction with BCL-2 family proteins underlies the proapoptotic activity of PUMA BH3. Chem Biol. 2013; 20:888–902. [PubMed: 23890007]

Fenstermacher SJ, Pazyra-Murphy MF, Segal RA. Campenot cultures and microfluidics provide complementary platforms for spatial study of dorsal root ganglia neurons. Microfluidic and …. 2015

Fukuda Y, Li Y, Segal RA. A Mechanistic Understanding of Axon Degeneration in Chemotherapy-Induced Peripheral Neuropathy. Frontiers in Neuroscience. 2017:11. [PubMed: 28174515]

Gavathiotis E, Suzuki M, Davis ML, Pitter K, Bird GH, Katz SG, Tu HC, Kim H, Cheng EH, Tjandra N, Walensky LD. BAX activation is initiated at a novel interaction site. Nature. 2008; 455:1076–1081. [PubMed: 18948948]

George EB, Glass JD, Griffin JW. Axotomy-induced axonal degeneration is mediated by calcium influx through ion-specific channels. The Journal of neuroscience : the official journal of the Society for Neuroscience. 1995; 15:6445–6452. [PubMed: 7472407]

Gornstein E, Schwarz T. The paradox of paclitaxel neurotoxicity: Mechanisms and unanswered questions. Neuropharmacology. 2014; (76 Pt A):175–183.

Gornstein EL, Schwarz TL. Neurotoxic mechanisms of paclitaxel are local to the distal axon and independent of transport defects. Experimental neurology. 2017; 288:153–166. [PubMed: 27894788]

Greenberg EF, Lavik AR, Distelhorst CW. Bcl-2 regulation of the inositol 1,4,5-trisphosphate receptor and calcium signaling in normal and malignant lymphocytes: potential new target for cancer treatment. Biochim Biophys Acta. 2014; 1843:2205–2210. [PubMed: 24642270]

Hotchkiss RS, McConnell KW, Bullok K, Davis CG, Chang KC, Schwulst SJ, Dunne JC, Dietz GP, Bahr M, McDunn JE, et al. TAT-BH4 and TAT-Bcl-xL peptides protect against sepsis-induced lymphocyte apoptosis in vivo. J Immunol. 2006; 176:5471–5477. [PubMed: 16622015]

Jin HW, Flatters SJ, Xiao WH, Mulhern HL, Bennett GJ. Prevention of paclitaxel-evoked painful peripheral neuropathy by acetyl-L-carnitine: effects on axonal mitochondria, sensory nerve fiber terminal arbors, and cutaneous Langerhans cells. Experimental neurology. 2008; 210:229–237. [PubMed: 18078936]

Kiya T, Kawamata T, Namiki A, Yamakage M. Role of satellite cell-derived L-serine in the dorsal root ganglion in paclitaxel-induced painful peripheral neuropathy. Neuroscience. 2011; 174:190–199. [PubMed: 21118710]

Konopleva M, Pollyea DA, Potluri J, Chyla B, Hogdal L, Busman T, McKeegan E, Salem AH, Zhu M, Ricker JL, et al. Efficacy and Biological Correlates of Response in a Phase II Study of Venetoclax

Monotherapy in Patients with Acute Myelogenous Leukemia. Cancer discovery. 2016; 6:1106–1117. [PubMed: 27520294]

Krols M, van Isterdael G, Asselbergh B, Kremer A, Lippens S, Timmerman V, Janssens S. Mitochondria-associated membranes as hubs for neurodegeneration. Acta Neuropathol. 2016; 131:505–523. [PubMed: 26744348]

LaBelle JL, Katz SG, Bird GH, Gavathiotis E, Stewart ML, Lawrence C, Fisher JK, Godes M, Pitter K, Kung AL, Walensky LD. A stapled BIM peptide overcomes apoptotic resistance in hematologic cancers. The Journal of clinical investigation. 2012; 122:2018–2031. [PubMed: 22622039]

Leshchiner ES, Braun CR, Bird GH, Walensky LD. Direct activation of full-length proapoptotic BAK. Proc Natl Acad Sci U S A. 2013; 110:E986–995. [PubMed: 23404709]

Li Y, Zhang H, Zhang H, Kosturakis AK, Jawad AB, Dougherty PM. Toll-like receptor 4 signaling contributes to Paclitaxel-induced peripheral neuropathy. J Pain. 2014; 15:712–725. [PubMed: 24755282]

Lovell JF, Billen LP, Bindner S, Shamas-Din A, Fradin C, Leber B, Andrews DW. Membrane binding by tBid initiates an ordered series of events culminating in membrane permeabilization by Bax. Cell. 2008; 135:1074–1084. [PubMed: 19062087]

Mincheva-Tasheva S, Obis E, Tamarit J, Ros J. Apoptotic cell death and altered calcium homeostasis caused by frataxin depletion in dorsal root ganglia neurons can be prevented by BH4 domain of Bcl-xL protein. Hum Mol Genet. 2014; 23:1829–1841. [PubMed: 24242291]

Mo M, Erdelyi I, Szigeti-Buck K, Benbow JH, Ehrlich BE. Prevention of paclitaxel-induced peripheral neuropathy by lithium pretreatment. FASEB journal : official publication of the Federation of American Societies for Experimental Biology. 2012; 26:4696–4709. [PubMed: 22889832]

Monaco G, Decrock E, Arbel N, van Vliet AR, La Rovere RM, De Smedt H, Parys JB, Agostinis P, Leybaert L, Shoshan-Barmatz V, Bultynck G. The BH4 domain of anti-apoptotic Bcl-XL, but not that of the related Bcl-2, limits the voltage-dependent anion channel 1 (VDAC1)-mediated transfer of pro-apoptotic Ca2+ signals to mitochondria. The Journal of biological chemistry. 2015; 290:9150–9161. [PubMed: 25681439]

Nakade S, Rhee SK, Hamanaka H. Cyclic AMP-dependent phosphorylation of an immunoaffinity-purified homotetrameric inositol 1, 4, 5-trisphosphate receptor (type I) increases Ca2+ flux in …. Journal of Biological …. 1994

Navarro SJ, Trinh T, Lucas CA, Ross AJ, Waymire KG, Macgregor GR. The C57BL/6J Mouse Strain Background Modifies the Effect of a Mutation in Bcl2l2. G3 (Bethesda). 2012; 2:99–102. [PubMed: 22384386]

Nikolaev A, McLaughlin T, O'Leary D, Tessier-Lavigne M. APP binds DR6 to trigger axon pruning and neuron death via distinct caspases. Nature. 2009; 457:981–989. [PubMed: 19225519]

Oakes SA, Opferman JT, Pozzan T, Korsmeyer SJ, Scorrano L. Regulation of endoplasmic reticulum Ca2+ dynamics by proapoptotic BCL-2 family members. Biochemical pharmacology. 2003; 66:1335–1340. [PubMed: 14555206]

Oakes SA, Scorrano L, Opferman JT, Bassik MC, Nishino M, Pozzan T, Korsmeyer SJ. Proapoptotic BAX and BAK regulate the type 1 inositol trisphosphate receptor and calcium leak from the endoplasmic reticulum. Proc Natl Acad Sci U S A. 2005; 102:105–110. [PubMed: 15613488]

Pachman DR, Barton DL, Watson JC, Loprinzi CL. Chemotherapy-Induced Peripheral Neuropathy: Prevention and Treatment. Clinical Pharmacology & Therapeutics. 2011

Pazyra-Murphy MF, Hans A, Courchesne SL, Karch C, Cosker KE, Heerssen HM, Watson FL, Kim T, Greenberg ME, Segal RA. A retrograde neuronal survival response: target-derived neurotrophins regulate MEF2D and bcl-w. The Journal of neuroscience : the official journal of the Society for Neuroscience. 2009; 29:6700–6709. [PubMed: 19458239]

Pease SE, Segal RA. Preserve and protect: maintaining axons within functional circuits. Trends in neurosciences. 2014; 37:572–582. [PubMed: 25167775]

Peters CM, Jimenez-Andrade JM, Jonas BM, Sevcik MA, Koewler NJ, Ghilardi JR, Wong GY, Mantyh PW. Intravenous paclitaxel administration in the rat induces a peripheral sensory neuropathy characterized by macrophage infiltration and injury to sensory neurons and their supporting cells. Experimental neurology. 2007a; 203:42–54. [PubMed: 17005179]

Peters CM, Jimenez-Andrade JM, Kuskowski MA, Ghilardi JR, Mantyh PW. An evolving cellular pathology occurs in dorsal root ganglia, peripheral nerve and spinal cord following intravenous administration of paclitaxel in the rat. Brain research. 2007b; 1168:46–59. [PubMed: 17698044]

Petros AM, Olejniczak ET, Fesik SW. Structural biology of the Bcl-2 family of proteins. Biochim Biophys Acta. 2004; 1644:83–94. [PubMed: 14996493]

Raturi A, Simmen T. Where the endoplasmic reticulum and the mitochondrion tie the knot: the mitochondria-associated membrane (MAM). Biochim Biophys Acta. 2013; 1833:213–224. [PubMed: 22575682]

Rong Y-PP, Bultynck G, Aromolaran AS, Zhong F, Parys JB, De Smedt H, Mignery GA, Roderick HL, Bootman MD, Distelhorst CW. The BH4 domain of Bcl-2 inhibits ER calcium release and apoptosis by binding the regulatory and coupling domain of the IP3 receptor. Proc Natl Acad Sci U S A. 2009; 106:14397–14402. [PubMed: 19706527]

Ross AJ, Waymire KG, Moss JE, Parlow AF, Skinner MK, Russell LD, MacGregor GR. Testicular degeneration in Bclw-deficient mice. Nat Genet. 1998; 18:251–256. [PubMed: 9500547]

Sasaki Y, Vohra BP, Lund FE, Milbrandt J. Nicotinamide mononucleotide adenylyl transferase-mediated axonal protection requires enzymatic activity but not increased levels of neuronal nicotinamide adenine dinucleotide. The Journal of neuroscience : the official journal of the Society for Neuroscience. 2009; 29:5525–5535. [PubMed: 19403820]

Schlaepfer WW, Bunge RP. Effects of calcium ion concentration on the degeneration of amputated axons in tissue culture. The Journal of cell biology. 1973; 59:456–470. [PubMed: 4805010]

Schoenmann Z, Assa-Kunik E, Tiomny S, Minis A, Haklai-Topper L, Arama E, Yaron A. Axonal degeneration is regulated by the apoptotic machinery or a NAD+-sensitive pathway in insects and mammals. The Journal of neuroscience : the official journal of the Society for Neuroscience. 2010; 30:6375–6386. [PubMed: 20445064]

Schulman JJ, Wright FA, Kaufmann T, Wojcikiewicz RJ. The Bcl-2 protein family member Bok binds to the coupling domain of inositol 1,4,5-trisphosphate receptors and protects them from proteolytic cleavage. J Biol Chem. 2013; 288:25340–25349. [PubMed: 23884412]

Scorrano L, Oakes SA, Opferman JT, Cheng EH, Sorcinelli MD, Pozzan T, Korsmeyer SJ. BAX and BAK regulation of endoplasmic reticulum Ca2+: a control point for apoptosis. Science (New York, NY). 2003; 300:135–139.

Shemesh OA, Spira ME. Paclitaxel induces axonal microtubules polar reconfiguration and impaired organelle transport: implications for the pathogenesis of paclitaxel-induced polyneuropathy. Acta neuropathologica. 2010; 119:235–248. [PubMed: 19727778]

Shimizu S, Konishi A, Kodama T, Tsujimoto Y. BH4 domain of antiapoptotic Bcl-2 family members closes voltage-dependent anion channel and inhibits apoptotic mitochondrial changes and cell death. Proc Natl Acad Sci U S A. 2000; 97:3100–3105. [PubMed: 10737788]

Siau C, Bennett GJ. Dysregulation of cellular calcium homeostasis in chemotherapy-evoked painful peripheral neuropathy. Anesthesia and analgesia. 2006; 102:1485–1490. [PubMed: 16632831]

Simon DJ, Pitts J, Hertz NT, Yang J, Yamagishi Y, Olsen O, Tesic Mark M, Molina H, Tessier-Lavigne M. Axon Degeneration Gated by Retrograde Activation of Somatic Pro-apoptotic Signaling. Cell. 2016; 164:1031–1045. [PubMed: 26898330]

Simon DJ, Weimer RM, McLaughlin T, Kallop D, Stanger K, Yang J, O'Leary DD, Hannoush RN, Tessier-Lavigne M. A caspase cascade regulating developmental axon degeneration. The Journal of neuroscience : the official journal of the Society for Neuroscience. 2012; 32:17540–17553. [PubMed: 23223278]

Sugioka R, Shimizu S, Funatsu T, Tamagawa H, Sawa Y, Kawakami T, Tsujimoto Y. BH4-domain peptide from Bcl-xL exerts anti-apoptotic activity in vivo. Oncogene. 2003; 22:8432–8440. [PubMed: 14627984]

Tang T-S, Tu H, Wang Z, Bezprozvanny I. Modulation of type 1 inositol (1, 4, 5)-trisphosphate receptor function by protein kinase A and protein phosphatase 1. Journal of Neuroscience. 2003; 23:403–415. [PubMed: 12533600]

Turkiew E, Falconer D, Reed N, Hoke A. Deletion of Sarm1 gene is neuroprotective in two models of peripheral neuropathy. J Peripher Nerv Syst. 2017; 22:162–171. [PubMed: 28485482]

Vanderheyden V, Devogelaere B, Missiaen L, De Smedt H, Bultynck G, Parys JB. Regulation of inositol 1,4,5-trisphosphate-induced Ca2+ release by reversible phosphorylation and dephosphorylation. Biochim Biophys Acta. 2009; 1793:959–970. [PubMed: 19133301]

Villegas R, Martinez NW, Lillo J, Pihan P, Hernandez D, Twiss JL, Court FA. Calcium release from intra-axonal endoplasmic reticulum leads to axon degeneration through mitochondrial dysfunction. The Journal of neuroscience : the official journal of the Society for Neuroscience. 2014; 34:7179–7189. [PubMed: 24849352]

Vohra B, Sasaki Y, Miller B, Chang J, DiAntonio A, Milbrandt J. Amyloid precursor protein cleavage-dependent and -independent axonal degeneration programs share a common nicotinamide mononucleotide adenylyltransferase 1-sensitive pathway. The Journal of neuroscience : the official journal of the Society for Neuroscience. 2010; 30:13729–13738. [PubMed: 20943913]

Wagner LE, Li W-HH, Yule DI. Phosphorylation of type-1 inositol 1,4,5-trisphosphate receptors by cyclic nucleotide-dependent protein kinases: a mutational analysis of the functionally important sites in the S2+ and S2− splice variants. The Journal of biological chemistry. 2003; 278:45811–45817. [PubMed: 12939273]

Wagner LE, Li WH, Joseph SK, Yule DI. Functional consequences of phosphomimetic mutations at key cAMP-dependent protein kinase phosphorylation sites in the type 1 inositol 1, 4, 5-trisphosphate …. Journal of Biological Chemistry. 2004

Walensky LD, Bird GH. Hydrocarbon-stapled peptides: principles, practice, and progress. J Med Chem. 2014; 57:6275–6288. [PubMed: 24601557]

Walensky LD, Kung AL, Escher I, Malia TJ, Barbuto S, Wright RD, Wagner G, Verdine GL, Korsmeyer SJ. Activation of apoptosis in vivo by a hydrocarbon-stapled BH3 helix. Science (New York, NY). 2004

Wang J, Medress Z, Barres B. Axon degeneration: molecular mechanisms of a self-destruction pathway. The Journal of cell biology. 2012; 196:7–18. [PubMed: 22232700]

Wang MS, Davis AA, Culver DG, Glass JD. WldS mice are resistant to paclitaxel (taxol) neuropathy. Annals of neurology. 2002; 52:442–447. [PubMed: 12325073]

Wang MS, Davis AA, Culver DG, Wang Q, Powers JC, Glass JD. Calpain inhibition protects against Taxol-induced sensory neuropathy. Brain : a journal of neurology. 2004; 127:671–679. [PubMed: 14761904]

Weyhenmeyer B, Murphy AC, Prehn JH, Murphy BM. Targeting the anti-apoptotic Bcl-2 family members for the treatment of cancer. Experimental oncology. 2012; 34:192–199. [PubMed: 23070004]

Yang IH, Siddique R, Hosmane S, Thakor N, Höke A. Compartmentalized microfluidic culture platform to study mechanism of paclitaxel-induced axonal degeneration. Experimental neurology. 2009; 218:124–128. [PubMed: 19409381]

Yang J, Wu Z, Renier N, Simon David J, Uryu K, Park David S, Greer Peter A, Tournier C, Davis Roger J, Tessier-Lavigne M. Pathological Axonal Death through a MAPK Cascade that Triggers a Local Energy Deficit. Cell. 2015; 160:161–176. [PubMed: 25594179]

Yilmaz E, Gold MS. Sensory neuron subpopulation-specific dysregulation of intracellular calcium in a rat model of chemotherapy-induced peripheral neuropathy. Neuroscience. 2015; 300:210–218. [PubMed: 25982563]

Zhang H, Yoon S-Y, Zhang H, Dougherty PM. Evidence that spinal astrocytes but not microglia contribute to the pathogenesis of Paclitaxel-induced painful neuropathy. The Journal of Pain. 2012; 13:293–303. [PubMed: 22285612]

Zong W-XX, Li C, Hatzivassiliou G, Lindsten T, Yu Q-CC, Yuan J, Thompson CB. Bax and Bak can localize to the endoplasmic reticulum to initiate apoptosis. The Journal of cell biology. 2003; 162:59–69. [PubMed: 12847083]

Highlights

- Paclitaxel acts directly on sensory axons to cause degeneration.
- Paclitaxel reduces translation of Bclw, a Bcl2 family member synthesized in axons.
- The Bclw BH4 domain specifically binds axonal IP_3R1 and prevents degeneration.

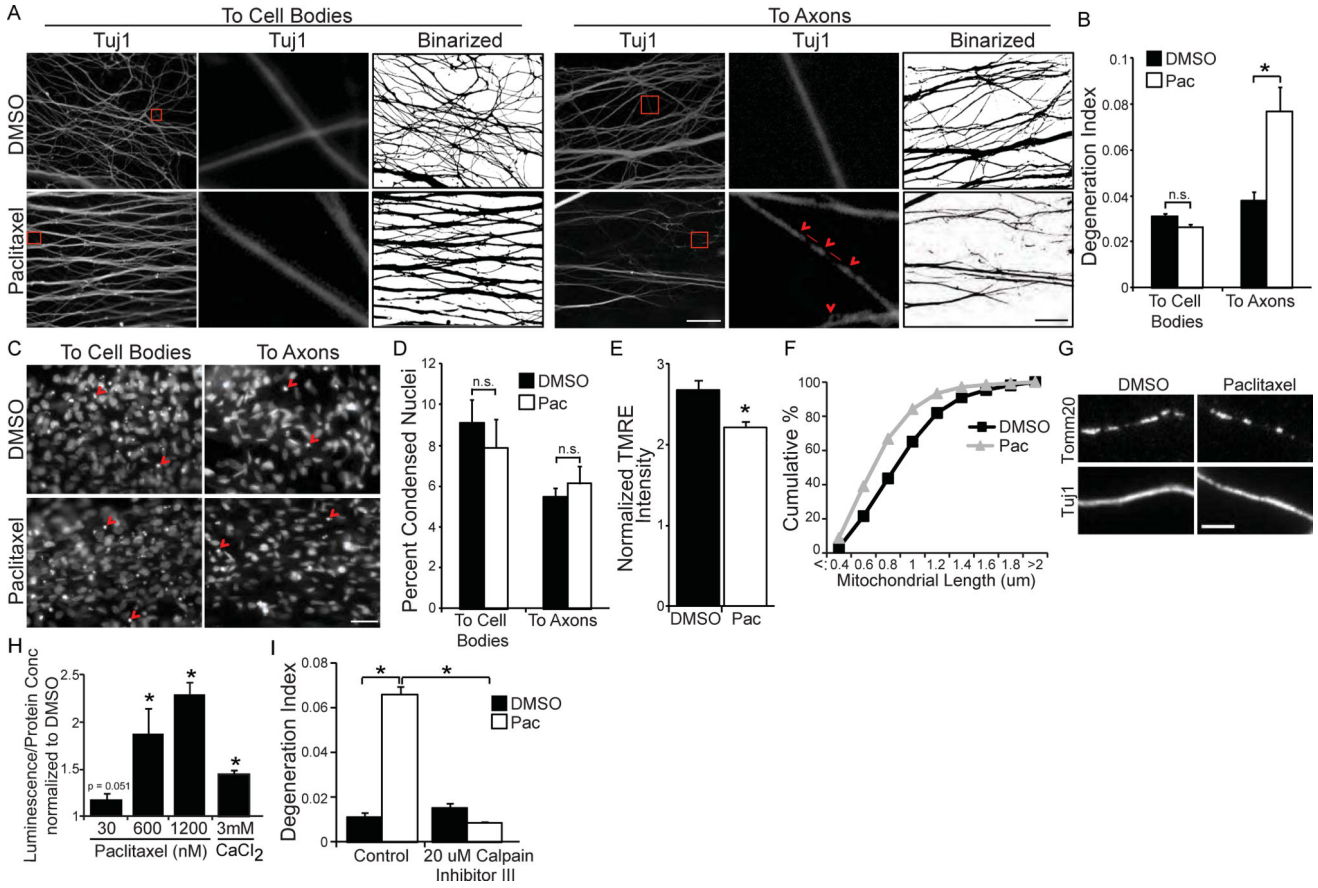

Figure 1. Paclitaxel acts locally to induce axon degeneration without cell body apoptosis

(A) Tuj1 immunostaining and corresponding binarized images of axons of E15 DRG neurons grown in compartmented cultures treated with 30 nM paclitaxel or DMSO vehicle control for 24 hours to cell body (left) or distal axon (right) compartments; scale bar = 40 μm. Red boxes outline regions shown at higher magnification in the center panels. Features characteristic of degenerating axons are seen: red arrowheads indicate a “beads on a string” appearance and the red lines indicate interruptions in Tuj1 continuity. (B) Quantification of axonal degeneration: ratio of area of fragmented axons to total axon area (degeneration index); *p<0.05 by Student’s *t*-test; n=3, data represent mean + SEM. (C) DAPI images of cell body compartments from (A); scale bar = 10 μm, red arrowheads indicate apoptotic nuclei. (D) Quantification of apoptotic/total nuclei after addition of paclitaxel or vehicle to cell bodies or distal axons; *p<0.05 by Student’s *t*-test; n=3; data represent mean + SEM; n.s = not significant. (E) Fluorescence intensity (Fm/Fc) of the voltage-sensitive dye TMRE in axons of DRG neurons in microfluidic cultures; 60 nM paclitaxel (Pac) or vehicle control added to distal axon compartment for 48 hours; *p<0.001 by Student’s *t*-test; n = 80 mitochondria across 3 experiments; data represent mean + SEM. (F) Distribution of axonal mitochondrial lengths visualized by Tomm20 immunostaining (G) of DRG neurons in microfluidic cultures; 60 nM paclitaxel or vehicle control added to distal axon compartment for 48 hours; n = 3 independent experiments (1049–1078 mitochondria). (H) Luminescence generated by calpain activity from DRG neurons treated for 48 hours with 30 nM, 600 nM, or 1.2 μM paclitaxel or for 24 hours with 3 mM calcium chloride. Luminescence normalized

to protein concentration and then data normalized to vehicle control; *p<0.05 by *z*-test; n=3; data represent mean + SEM. (I) Degeneration index of axons treated with paclitaxel or vehicle control in the absence or presence of 20 μM calpain inhibitor III to axons; *p<0.05 by one-way ANOVA with Bonferroni correction; n=3; data represent mean + SEM.

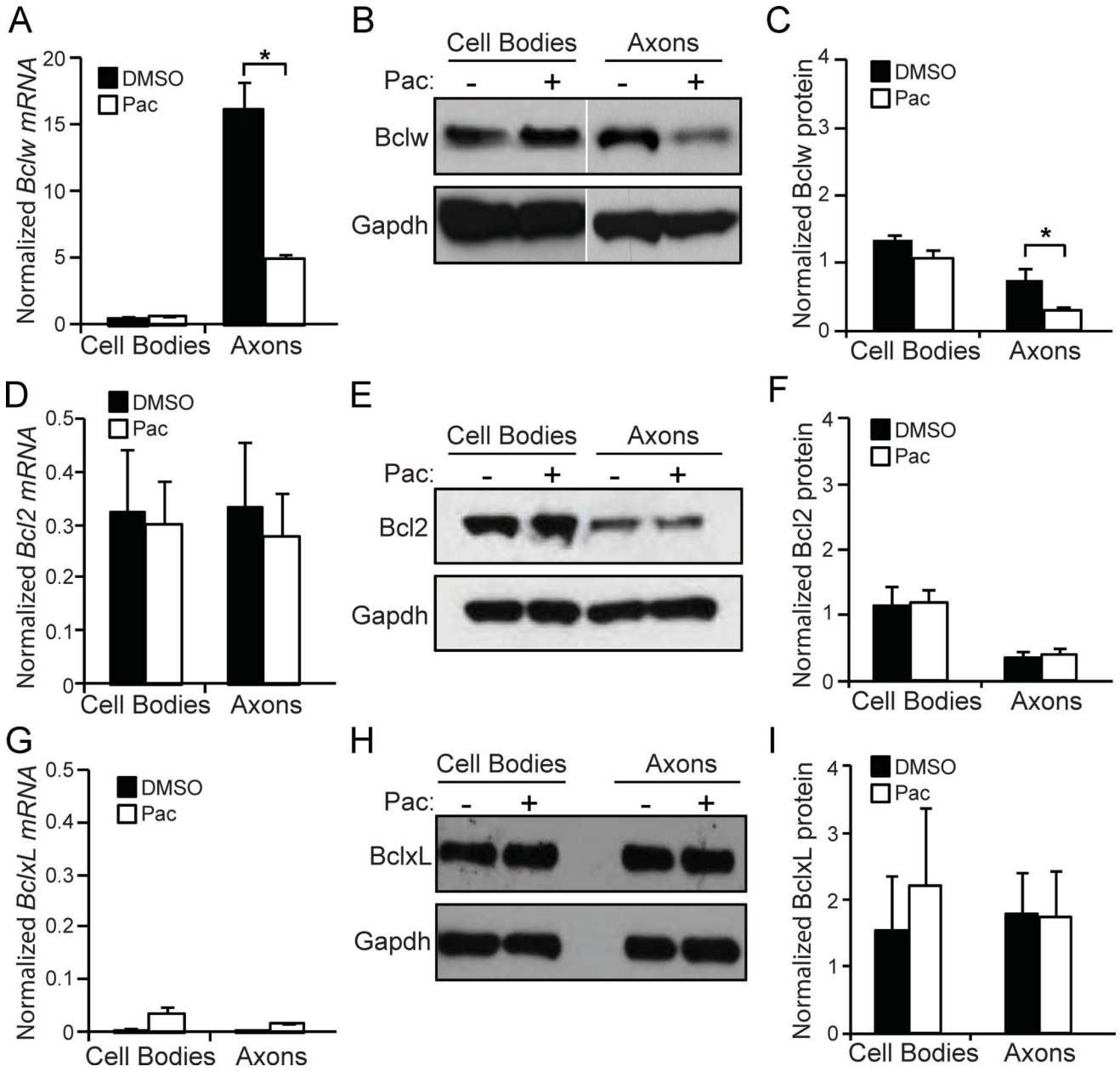

Figure 2. Paclitaxel reduces axonal Bclw mRNA and protein levels

bclw (A), *bcl2* (D) and *bclx*$_L$ (G) mRNA analyzed by qRT-PCR from cell body or axon lysate of compartmented cultures after 24 hours of paclitaxel or vehicle treatment to axons. Data normalized to *gapdh*; *p<0.05 by one-way ANOVA with Bonferroni correction; n=3; data represent mean + SEM. Western blot of protein for Bclw (B, C), Bcl2 (E, F), and Bclx$_L$ (H, I) and quantification from cell body or distal axon lysate of compartmented cultures after 24 hours of paclitaxel treatment to axons; data normalized to GAPDH; *p<0.05 by one-way ANOVA with Bonferroni correction; n=3; data represent mean + SEM.

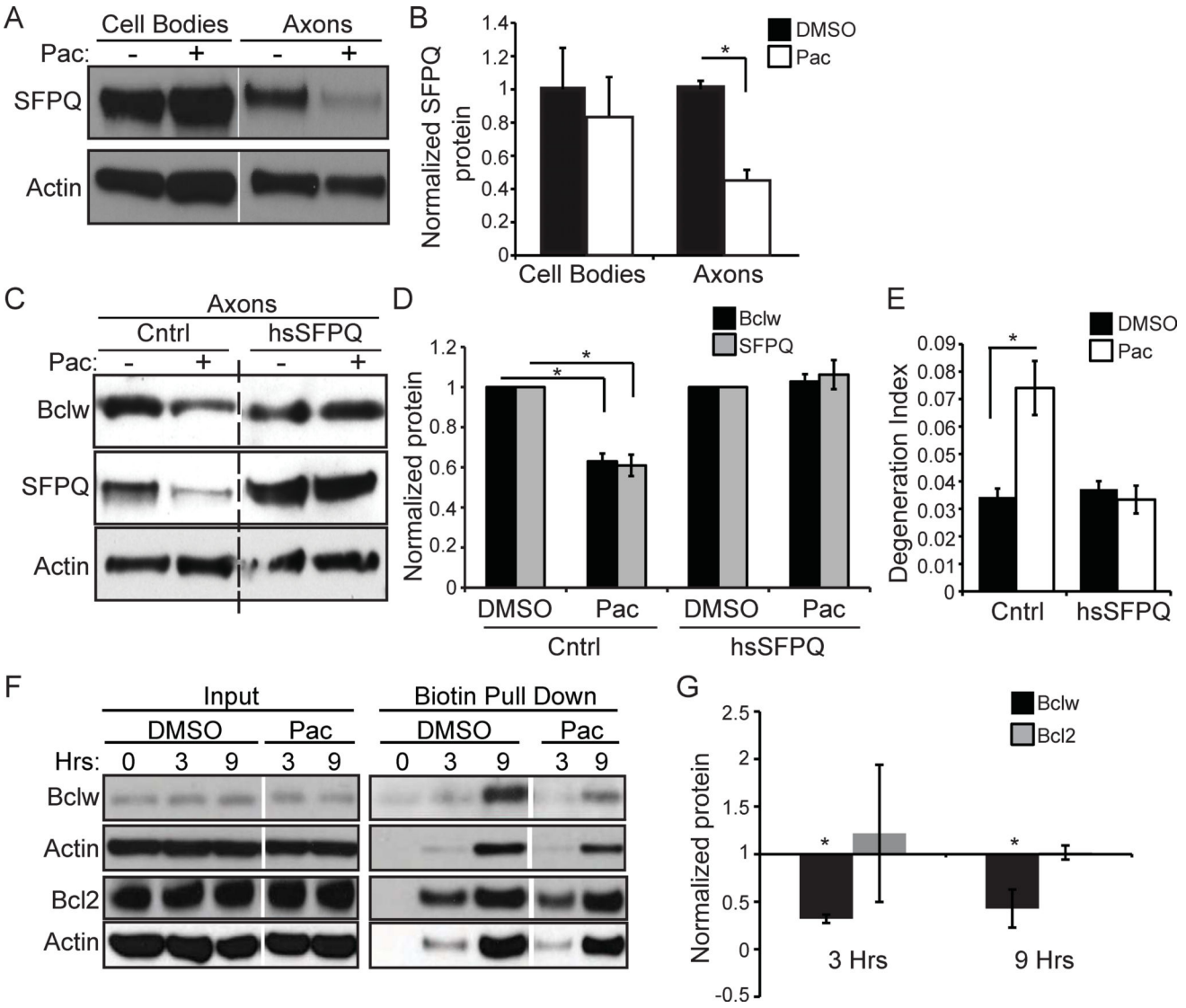

Figure 3. Paclitaxel reduces translation of Bclw via reduction of SFPQ

(A) Western blot and (B) quantification of SFPQ protein from cell body or distal axon lysate of compartmented cultures after 24 hours of paclitaxel treatment to axons; data normalized to actin; *p<0.05 by Student's *t*-test; n=3; data represent mean + SEM. (C) Western blot and (D) quantification of Bclw and SFPQ protein from distal axon lysate of compartmented cultures after 24 hours of paclitaxel treatment to axons following infection with a SFPQ-expressing (hsSFPQ) or control (Cntrl) lentivirus; data normalized to actin; *p<0.05 by one-way ANOVA with Bonferroni correction; n=3; data represent mean ± SEM. See also Figure S1. (E) Degeneration index of axons treated with paclitaxel or vehicle following infection with hsSFPQ or Cntrl lentivirus; *p<0.05 by one-way ANOVA; n=3 independent experiments (20–25 images); data represent mean ± SEM. (F) Western blot and (G) quantification of Bclw, Bcl2, or actin proteins showing input lysate and biotin pulldown of newly synthesized proteins in mass cultures after 0, 3, or 9 hours of simultaneous AHA labeling and paclitaxel or DMSO vehicle control treatment; data normalized to vehicle

control; *p<0.05 by ztest; n=4; data represent mean ± SEM; samples for control and paclitaxel were run on same gel and are from the same exposure.

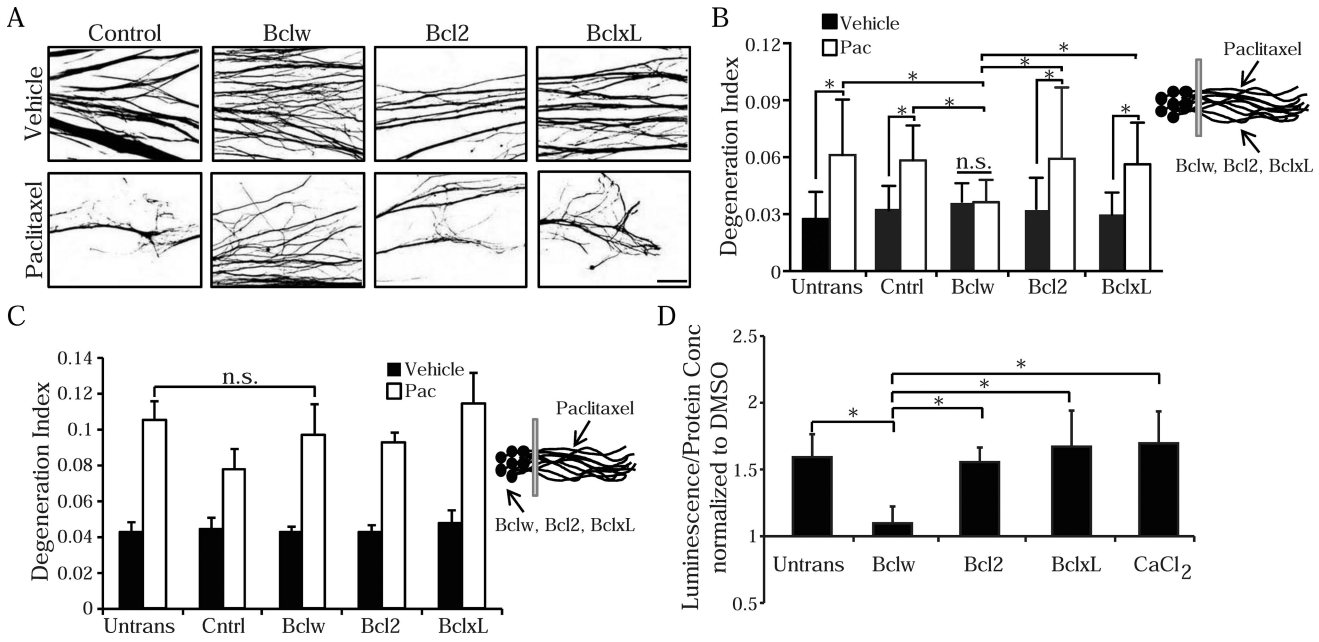

Figure 4. Axonal Bclw prevents paclitaxel-induced degeneration

(A) Binarized images of Tuj1 immunostaining of axons treated with paclitaxel or vehicle after protein transfection with Bclw, Bcl2, $Bclx_L$ or β-galactosidase control protein into axons; scale bar = 40 μm. See also Figure S2. (B) Degeneration index of (A) and untransfected (Untrans) control; *p<0.05 by one-way ANOVA; n.s. = not significant; n=6 independent experiments (30–35 images); data represent mean + SEM. (C) Degeneration index of axons treated with paclitaxel or vehicle after protein transfection of Bclw, Bcl2, $Bclx_L$ or β-galactosidase control protein into cell bodies; *p<0.05 by one-way ANOVA; n=4 independent experiments (20–25 images); data represent mean + SEM. (D) Calpain activity from DRG neurons untransfected or transfected with Bclw, Bcl2, or $Bclx_L$ protein and then treated for 24 hours with 600 nM paclitaxel, vehicle, or 3 mM calcium chloride. Luminescence readout normalized to protein concentration and then data normalized to vehicle control; *p<0.05 by Student's *t*-test; n=9–12 cultures; data represent mean + SEM.

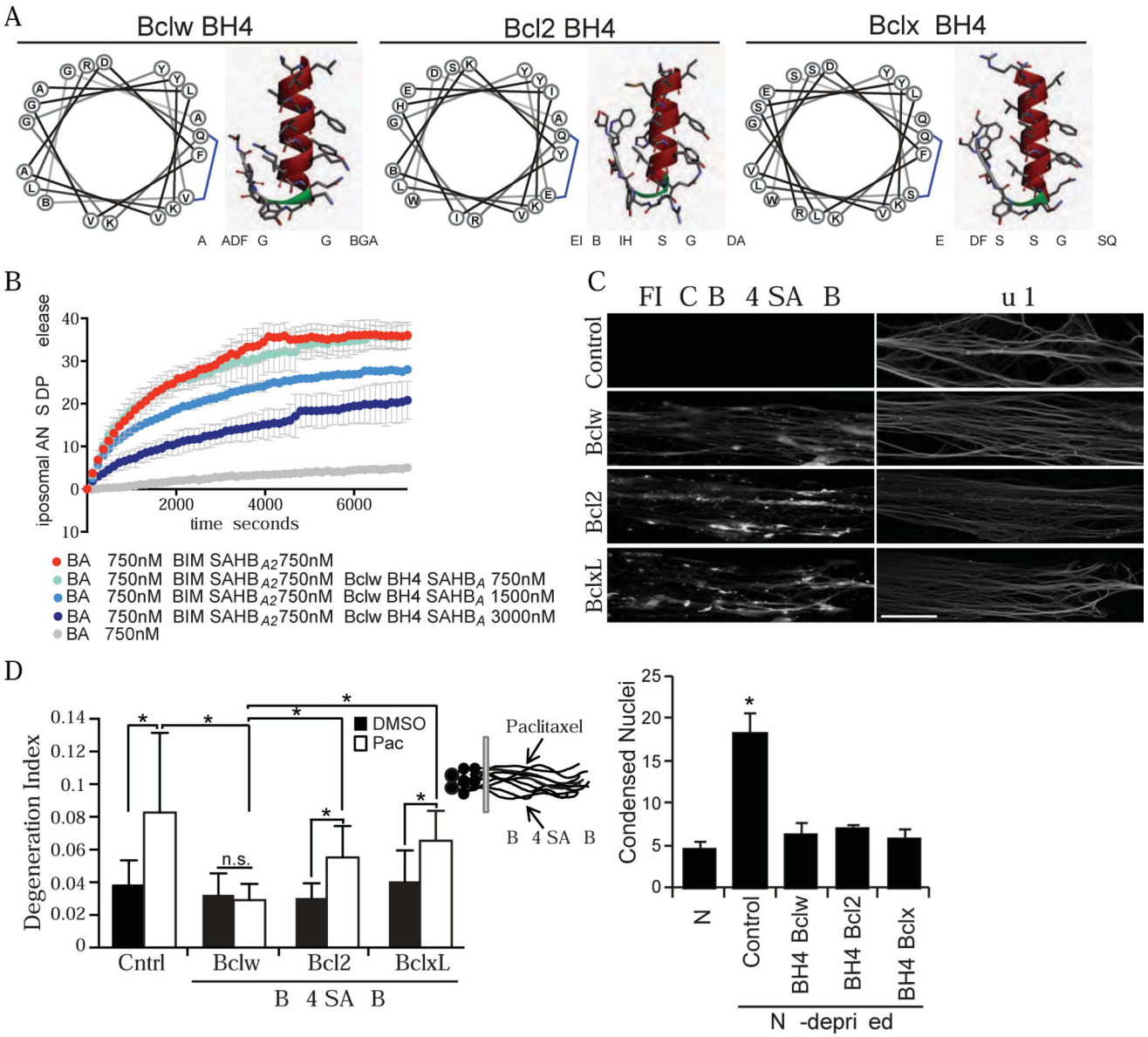

Figure 5. The Bclw BH4 domain is sufficient to prevent paclitaxel-induced axon degeneration

(A) Schematic of stabilized alpha-helix of Bcl2 domain (SAHB) peptides modeled after the BH4 domains of Bclw (PDB ID 4CIM, aa 12-31), Bcl2 (PDB ID 2XA0, aa 13-32), and $Bclx_L$ (PDB ID 4QVE, aa 6-26). (B) Percent release of ANTS/DPX encapsulated liposomes in the presence of Bax, Bim $SAHB_{A2}$, and/or Bclw BH4 $SAHB_A$ as indicated; n=3; data represent mean ± SD. (C) Axons from compartmented cultures after protein transfection with FITC-BH4 SAHB peptides of Bclw, Bcl2, or $Bclx_L$ showing FITC signal (left) and Tuj1 signal (right); scale bar = 20 μm. (D) Degeneration index of axons treated with paclitaxel or DMSO after protein transfection of FITC-BH4 SAHB-Bclw, Bcl2, or $Bclx_L$ into axons; *p<0.05 by one-way ANOVA with Bonferroni correction, n.s. = not significant; n=6 independent experiments (30–35 images); data represent mean + SEM. (E) Apoptotic/ total DAPI-stained nuclei of neurons maintained in neurotrophins (NT) or deprived of neurotrophins, cell bodies were transfected with FITC-BH4 SAHB peptides of Bclw, Bcl2,

or $Bclx_L$; *p<0.05 by one-way ANOVA with Bonferroni correction; n=4; data represent mean + SEM.

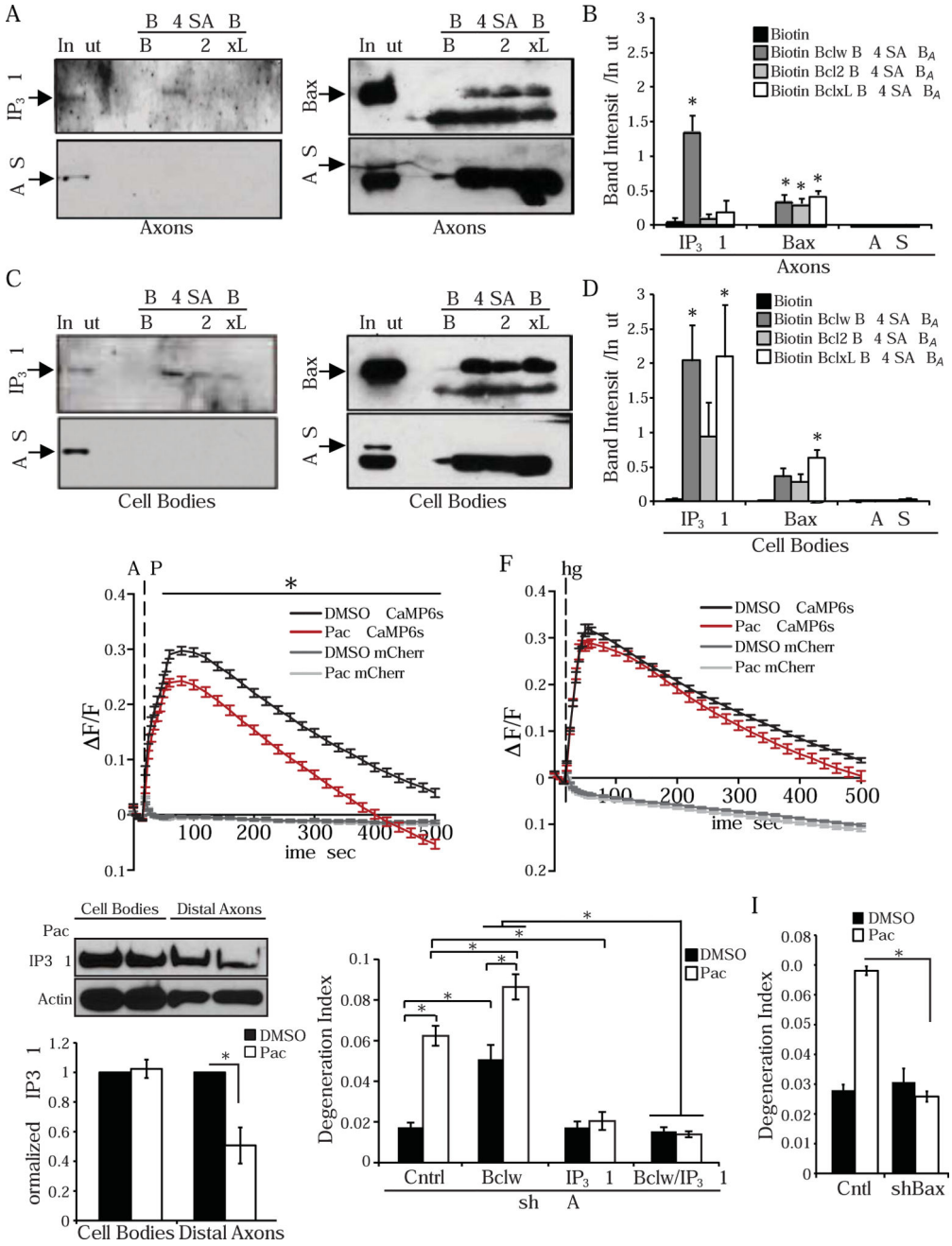

Figure 6. Bclw binds IP$_3$R1 to prevent axon degeneration

(A-D) Western blot of NeutrAvidin pulldowns from axon (A) or cell body (C) lysate incubated with biotinylated Bclw BH4 SAHB$_A$ (W), Bcl2 BH4 SAHB$_A$ (2), or Bclx$_L$ BH4 SAHB$_A$ (x$_L$) or biotin control (B). Western blots probed for IP$_3$R1, Bax, or YARS protein. (B) Quantified band intensity relative to input band from (A). (D) Quantified band intensity relative to input band from (C); *p<0.05 relative to biotin control by one-way ANOVA with Dunnett's multiple comparison test; n=4–6; data represent mean + SEM; # indicates nonspecific band. (E) Change in fluorescence intensity (ΔF/F) of GCaMP6s or mCherry signal from DRG neurons stimulated with 200 μM ATP (zero extracellular calcium media

+ 10 mM EGTA), after 600 nM paclitaxel or vehicle control added to culture for 24 hours; *p<0.05 by two-way ANOVA with Bonferroni correction; n = 119 (paclitaxel) or 156 (vehicle) cell bodies from 3 cultures across 3 experiments; data represent mean ± SEM. (F) Change in fluorescence intensity (ΔF/F) of GCaMP6s or mCherry signal from DRG neurons stimulated with 5 μM thapsigargin (zero extracellular calcium media + 10 mM EGTA), after 600 nM paclitaxel or vehicle control added to culture for 24 hours; *p<0.05 by two-way ANOVA with Bonferroni correction; n = 196 (paclitaxel) or 233 (vehicle) cell bodies from 3 cultures across 3 experiments; data represent mean ± SEM. (G) Western blot and quantification of p-IP_3R1 from cell body and axonal lysates treated with DMSO or paclitaxel, data normalized to actin; *p<0.05 by one-way ANOVA with Bonferroni correction; n=3; data represent mean ± SEM. (H) Degeneration index after 24 hours of paclitaxel or DMSO added to axons following lentiviral infection with shRNA targeting Bclw, IP_3R1, or control shRNA; *p<0.05 by one-way ANOVA with Bonferroni correction; n=3 independent experiments (20–25 images); data represent mean ± SEM. See also Figure S3B and S3C. (I) Degeneration index after 24 hours of paclitaxel or DMSO added to axons following lentiviral infection with shRNA targeting Bax or control shRNA; *p<0.05 by one-way ANOVA with Bonferroni correction; n=3 independent experiments (20–25 images); data represent mean ± SEM. See also Figure S3D.

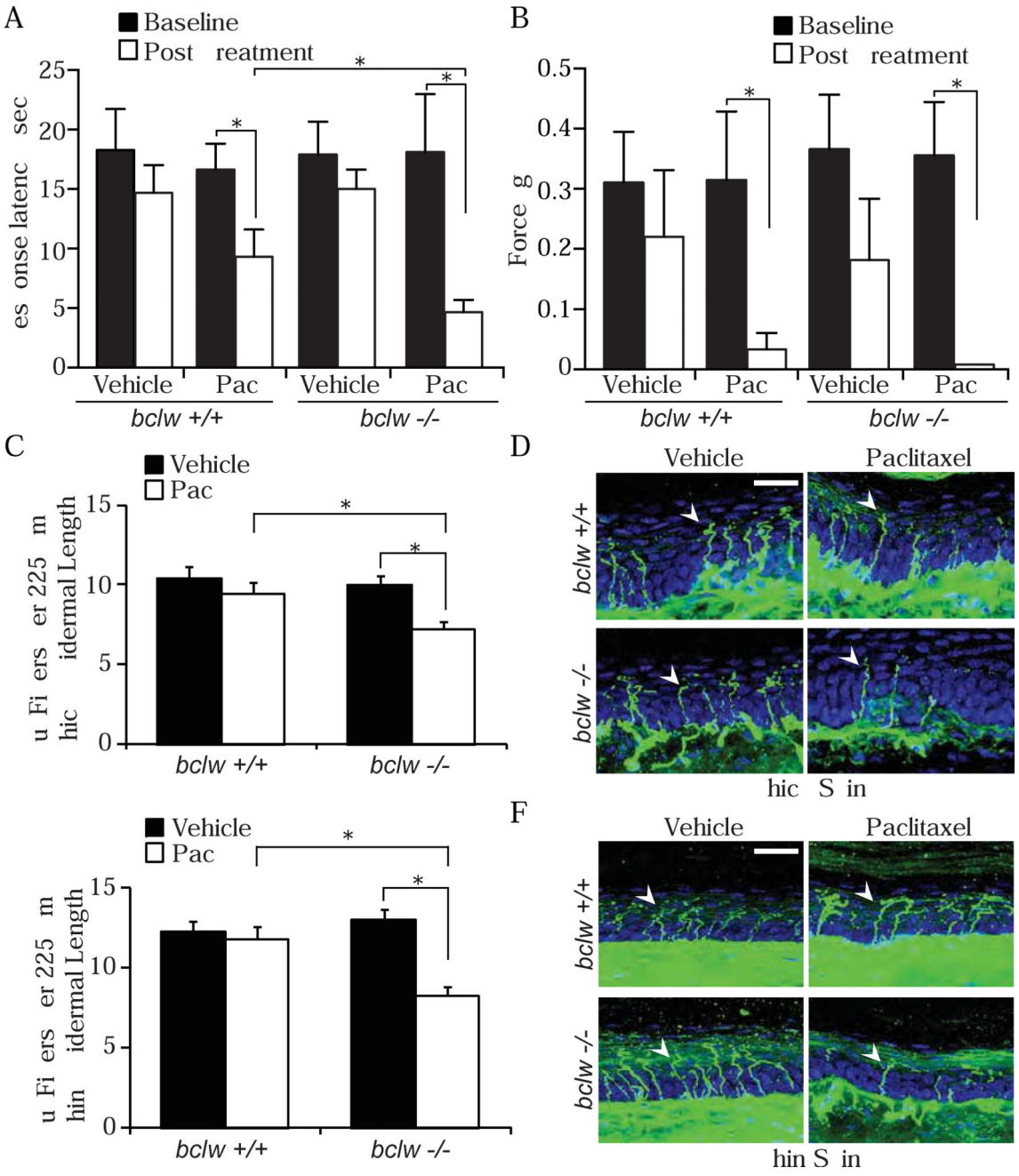

Figure 7. Loss of Bclw exacerbates paclitaxel-induced neuropathy *in vivo*

(A-B) Behavioral assessments of mice before (Baseline) and ten days after the final injection (Post Treatment) of paclitaxel or vehicle control; *p<0.05 by one-way ANOVA with Bonferroni correction, data represent mean + SEM, n=4–7 mice; data represent mean + SEM. See also Figure S5. (A) Thermal pain threshold measured as time to lick or withdraw hindpaw on a 50°C hot-plate. (B) Mechanical pain threshold determined from response to von Frey filaments. (C-F) Quantification and representative images of Tuj1 positive sensory fibers (green, arrowheads) entering the epidermis per 225 μm epidermal length in thick (C-D) and thin (E-F) skin, DAPI counterstain (blue); scale bar = 25 μm; *p<0.05 by one-way

ANOVA with Bonferroni correction; n=3–4 mice, 8–15 images per mouse; data represent mean + SEM.

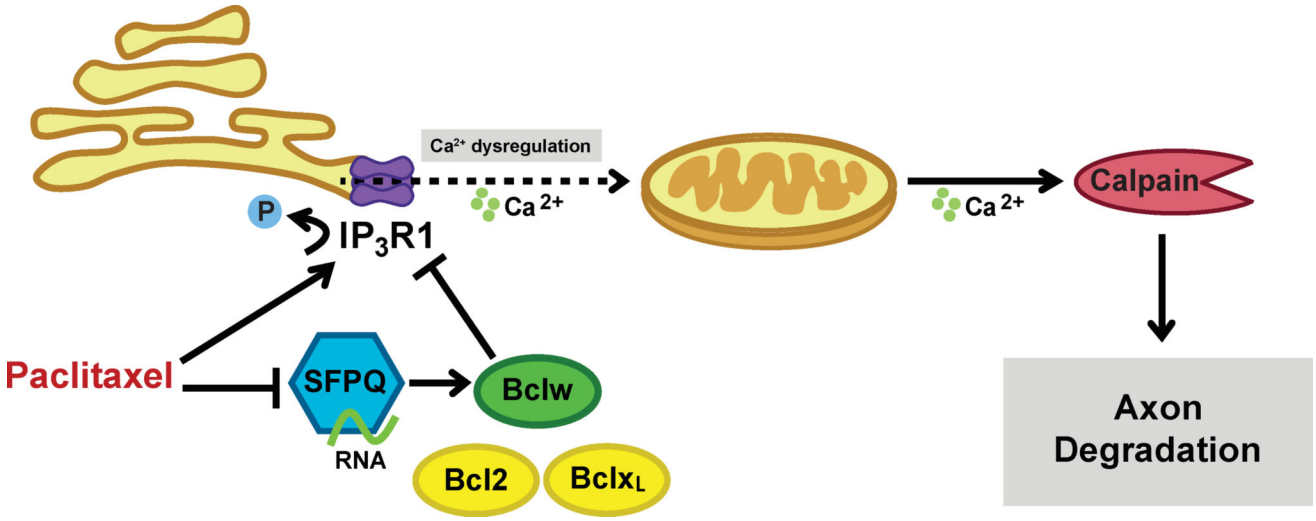

Figure 8. Model for paclitaxel-induced degeneration

Paclitaxel-induced microtubule stabilization decreases transport of SFPQ RNA granules containing *bclw* mRNA, thereby reducing axonal Bclw levels and dysregulating IP_3R1, resulting in activation of a degeneration cascade characterized by mitochondrial dysfunction and proteolysis by a calcium-dependent enzyme, calpain.